Formal Analysis of the Sampling Behavior of Stochastic Event-Triggered Control

Delimpaltadakis, Giannis; Laurenti, Luca; Mazo, Manuel

DOI
10.1109/TAC.2023.3333748

Publication date
2024

Document Version
Final published version

Published in
IEEE Transactions on Automatic Control

Formal Analysis of the Sampling Behavior of Stochastic Event-Triggered Control

Giannis Delimpaltadakis, *Member, IEEE*, Luca Laurenti, and Manuel Mazo Jr., *Senior Member, IEEE*

***Abstract*—Analyzing event-triggered control's (ETC) sampling behavior is of paramount importance, as it enables formal assessment of its sampling performance and prediction of its sampling patterns. In this work, we formally analyze the sampling behavior of stochastic linear periodic ETC (PETC) systems by computing bounds on associated metrics. Specifically, we consider functions over sequences of state measurements and intersampling times that can be expressed as average, multiplicative or cumulative rewards, and introduce their expectations as metrics on PETC's sampling behavior. We compute bounds on these expectations, by constructing Interval Markov Chains equipped with suitable reward functions, that abstract stochastic PETC's sampling behavior. Our results are illustrated on a numerical example, for which we compute bounds on the expected average intersampling time and on the probability of triggering with the maximum possible intersampling time in a finite horizon.**

***Index Terms*—Bounded-parameter Markov decision processes, event-triggered control, finite abstractions, interval Markov decision processes, networked control systems, stochastic systems.**

I. Introduction

In THE past two decades, event-triggered control (ETC) has constituted the primary research focus of the control systems community toward reducing resource consumption in networked control systems [1], [2], [3], [4], [5], [6], [7], [8], [9], [10], [11], [12], [13], [14], [15], [16], [17], [18], [19], [20], [21], [22]. ETC is a sampling paradigm, where communication between the sensors and the controller takes place only when a state-dependent triggering condition is satisfied. Even though ETC's event-based sampling typically reduces the amount of communications (compared to conventional periodic sampling), it also generates an erratic and generally a priori unknown *sampling behavior*; given an ETC system, the times at which communication is going to take place are not known beforehand. Obtaining information on ETC's sampling behavior and predicting its communication (or sampling) patterns is crucial, as it enables: a) formally assessing an ETC design's sampling performance (e.g., determining how frequently the system is expected to sample, which quantifies expected energy and bandwidth savings), and b) scheduling communication traffic[1] in networks shared by multiple ETC loops, to avoid packet collisions and thus facilitate deployment of ETC systems in congested networks.

Although analyzing ETC's sampling behavior is fundamental, research around it is scarce [9], [10], [11], [12], [13], [14], [15], [16], [17], [18]. One branch of it composes of analytic approaches [9], [10], [11], [12], [13]. In particular, Demirel et al. [9] studied deadbeat stochastic linear PETC (periodic ETC, e.g., [2]; a practical variant of ETC[2]) systems. Owing to deadbeat control, studying the sampling behavior of the system simplifies to analyzing a Markov chain, which can be used to compute quantitative metrics over the sampling performance. Nevertheless, assuming deadbeat control is admittedly restrictive. Similarly, authors in [10] and [11] perform analytic studies on ETC's expected average *intersampling time*, but again rely on simple system dynamics (assuming that the controller can reset the state to 0) and it is not clear if these results may be extended to more general metrics on ETC's sampling. Further, authors in [12] and [13] derive interesting results on asymptotic properties of the intersampling times of 2-D linear ETC systems with quadratic triggering conditions. However, they also obey certain limitations: they 1) address only planar systems, 2) are dependent on the type of triggering condition considered, and most importantly 3) do not provide quantitative information on all possible sampling patterns that may be exhibited by an ETC system; as such, they cannot be employed to compute metrics on ETC's sampling performance or predict its sampling patterns. Finally, some works design ETC schemes to optimize performance criteria involving sampling-related metrics (typically, average intersampling time), e.g., [19], [20], [21], [22]; however,

Manuscript received 19 September 2022; revised 8 June 2023 and 1 November 2023; accepted 11 November 2023. Date of publication 17 November 2023; date of current version 28 June 2024. This work was supported by ERC Starting Grant SENTIENT (755953). Recommended by Associate Editor Z. Li. *(Corresponding author: Giannis Delimpaltadakis.)*

Giannis Delimpaltadakis is with the Control Systems Technology section, Mechanical Engineer, Eindhoven University of Technology, 5600 MB Eindhoven, The Netherlands (e-mail: i.delimpaltadakis@tue.nl).

Luca Laurenti and Manuel Mazo are with the Delft Center for Systems and Controls, Delft University of Technology, 2628 CD Delft, The Netherlands (e-mail: l.laurenti@tudelft.nl; m.mazo@tudelft.nl).

Digital Object Identifier 10.1109/TAC.2023.3333748

[1]Traffic scheduling is much more trivial with periodic sampling, where the generated traffic is known beforehand.

[2]In PETC, the triggering condition is checked only periodically, as opposed to CETC, where this happens continuously in time. As such, the framework of PETC models practical scenarios more realistically, since (see, e.g., [2]): a) in practice, checking the triggering condition is performed by smart sensors, which generally operate digitally, and b) in most networks, communication takes place in discrete time instants.

this is not in this article's scope, which focuses on analyzing the sampling behavior of a given ETC system.

The other branch of research studying ETC's sampling behavior is *abstraction*-based approaches [14], [15], [16], [17], [18], among which the present work is placed. These construct finite-state systems, abstracting a given ETC system's sampling: The set of their traces contains all possible sequences of intersampling times that may be exhibited by the ETC system. Contrary to the analytic approaches, they do not place restrictive assumptions on system dynamics, system dimensions (modulo computational complexity), and the triggering condition (except that minor steps in the abstraction's construction might vary). Meanwhile, in exchange for high computational complexity, they provide quantitative information on ETC's diverse sampling patterns, allowing for computing performance metrics and predicting sampling patterns. For example, the work in [15], [16], [17], and [18] constructed abstractions for ETC traffic scheduling, while Gleizer and Mazo [14] utilized them to compute the minimum average intersampling time.

Thus far, in [15], [16], [14], [17], and [18] only nonstochastic systems have been considered. Specifically, authors in [14], [15], and [16] considered linear ETC and PETC systems, whereas in [17] and [18] addressed nonlinear systems with bounded disturbances. In this work, we consider *stochastic* systems, for the first time. Among others, for verification purposes, the probabilistic framework of stochastic systems is naturally less strict than the deterministic one, as it takes into account the disturbances' probability distribution, instead of being bound by worst-case scenarios.

In particular, we consider stochastic linear PETC systems. We define their sampling behavior as the set Y of all possible sequences of state-measurements and intersampling times along with its associated probability measure. Studying ETC's sampling behavior is formalized by computing expectations of functions defined over these sequences $g : \mathrm{Y} \to \mathbb{R}$. Here, we focus on functions g described as cumulative, average, or multiplicative rewards, i.e., $g_\star$ with $\star \in \{\mathrm{cum}, \mathrm{avg}, \mathrm{mul}\}$. This class of functions is rather standard in the context of quantitative analysis of stochastic systems, and it extends to including specifications of probabilistic computation tree logic (PCTL; see [23]). Besides, it is able to describe various metrics on ETC's sampling performance, as demonstrated through examples in Section III-B. In fact, as shown in one example, including state-measurements in the sampling behavior's definition allows for incorporating control-performance metrics as well. The problem statement of this work is to obtain bounds on expectations of functions $g_\star$.

To address the problem, given a PETC system, we construct an IMC (interval Markov chain; Markov chain with interval transition probabilities) that captures its sampling behavior. Then, we equip the IMC with appropriate reward functions and prove that the $\{\mathrm{cum}, \mathrm{avg}, \mathrm{mul}\}$ rewards over the paths of the IMC indeed bound the expectation of $g_\star$ (see Theorem IV.1). The IMC rewards can easily be computed via well-known value-iteration algorithms (see, e.g., [24]).

The main challenge in constructing the IMC is computing the IMC's probability intervals. For that, we study the joint probabilities of transitioning from one region of the state-space to another and the intersampling time taking a specific value. Computation of these probabilities is more complicated than the traditional transition probabilities that appear in the literature of IMC-abstractions (e.g., [23], [25], [26], [27]), due to the presence of intersampling time as an event. To cope with that, we employ a series of convex relaxations and the fact that the system's state is a Gaussian process. That way, we reformulate computing these probabilities as optimization problems of log-concave objective functions and hyperrectangle constraint sets, which are easy to solve. Finally, our results are demonstrated through a numerical example, where we compute bounds on the expected average intersampling time and on the probability of triggering with the maximum possible intersampling time in a finite horizon, for a given system.

In summary, this work's main contributions are as follows.

1) It is the first one to abstract the sampling behavior of stochastic ETC.
2) It computes bounds on performance metrics over stochastic PETC's sampling behavior, allowing for its formal assessment and prediction of its patterns.

A preliminary version of the present work was presented in [28]. In [28], only cumulative rewards are addressed and the derived upper and lower bounds on transition probabilities are different (here, they are tighter). Furthermore, the proof of Lemma V.2, which shows log-concavity of our optimization problems' objective functions, appears here for the first time. Finally, as Theorem IV.1 argues about any horizon, its proof, employing time-varying adversaries, is more elaborate than the proof of [28, Th. IV.1], which argues only about infinite horizons, where time-invariant adversaries suffice.

II. Preliminaries

A. Notation

$\mathbb{R}$ stands for the set of real numbers, $\mathbb{N}$ for the natural numbers including 0, and $\mathbb{N}_+$ without 0. Given a vector $x \in \mathbb{R}^n$, we denote $|x|_\infty \equiv \max_i |x_i|$, where x_i is the ith component of the vector. Given $X \subseteq \mathbb{R}$, $X_{[a,b]} = X \cap [a, b]$. I_n is the n-dimensional identity matrix. Given a set S in some space X, we denote: its indicator function by $\mathbb{1}_S(\cdot)$, its Borel σ-algebra by $\mathcal{B}(S)$, its complement by $\overline{S} = X \setminus S$, and the k-times Cartesian product $S = S \times \cdots \times S$ by S^k. Given $x \in \mathbb{R}^n$, denote by $\{x\}^k$: Both the k-times Cartesian product $\{x\} \times \cdots \times \{x\}$ and the kn-dimensional vector $\begin{bmatrix} x^\top & \dots & x^\top \end{bmatrix}^\top$. Given sets Q_1, Q_2, and $Q = Q_1 \times Q_2$, for any $q = (q_1, q_2) \in Q$ denote $\mathbf{proj}_{Q_1}(q) = q_1$ and $\mathbf{proj}_{Q_2}(q) = q_2$. Given two sets Q_1, Q_2 in some space, denote $Q_1 + Q_2 = \{q_1 + q_2 : q_1 \in Q_1, q_2 \in Q_2\}$ and $Q_1 - Q_2 = \{q_1 - q_2 : q_1 \in Q_1, q_2 \in Q_2\}$. Consider a parameter-dependent set $S(x) \subseteq \mathbb{R}^n$, where $x \in \mathbb{R}^m$ (i.e., a set-valued function $S : \mathbb{R}^m \to 2^{\mathbb{R}^n}$). We say that $S(x)$ is *linear on* x, if $S(x) = S' + \{Ax\}$, where $A \in \mathbb{R}^{n \times m}$ and $S' \subseteq \mathbb{R}^n$.

Given a random variable x and an associated probability measure $\mathbb{P}$, we denote its expectation w.r.t. $\mathbb{P}$ by $\mathrm{E}_{\mathbb{P}}[x]$ (when $\mathbb{P}$ is clear from the context, it might be omitted). We use the term "path" or "sequence" interchangeably. Given a finite path $\omega = q_0, q_1 \dots, q_N$, denote $\omega(i) = q_i$ and $\omega(end) = \omega(N) = q_N$. Given a function $g(\omega)$ of paths ω, we denote

$\mathrm{E}^{q_0}[g(\omega)] \equiv \mathrm{E}[g(\omega)|\omega(0) = q_0]$. Finally, $\mathcal{N}(\mu, \Sigma)$ denotes the Gaussian distribution with mean μ and covariance matrix Σ.

B. Rewards Over Paths

Consider a set Q and a set of paths Y of length $N+1$, such that: $\omega(i) \in Q$, for all $\omega \in \mathrm{Y}$ and $0 \leq i \leq N$. Assume a probability measure $\mathbb{P}$ over $\mathcal{B}(\mathrm{Y})$ (for how to define $\mathcal{B}(\mathrm{Y})$ in our context, see Section III-B). Define a *reward function* $R : Q \to [0, R_{\max}]$. We define the following expectations:

1) *Cumulative (discounted) reward:* $\mathrm{E}_{\mathbb{P}}[g_{\mathrm{cum},N}(\omega)] \equiv \mathrm{E}_{\mathbb{P}}[\sum_{i=0}^{N} \gamma^i R(\omega(i))]$, where $\gamma \in [0, 1]$.
2) *Average reward:* $\mathrm{E}_{\mathbb{P}}[g_{\mathrm{avg},N}(\omega)] \equiv \mathrm{E}_{\mathbb{P}}[\frac{1}{N+1} \sum_{i=0}^{N} R(\omega(i))]$.
3) *Multiplicative reward:* $\mathrm{E}_{\mathbb{P}}[g_{\mathrm{mul},N}(\omega)] \equiv \mathrm{E}_{\mathbb{P}}[\prod_{i=0}^{N} R(\omega(i))]$.

These expectations can describe a wide range of quantitative/qualitative properties of paths in Y, and they have been employed for verification in numerous settings, such as (interval) Markov chains (e.g., [23], [25], [26], [27]), stochastic hybrid systems (e.g., [29]), etc. Later, we showcase their descriptive power within our framework (see Section III-B).

C. Interval Markov Chains (IMCs)

IMCs are Markov models with interval transition probabilities, and they are defined as:

Definition II.1 (IMC): *An IMC is a tuple* $\mathrm{S}_{imc} = \{Q, \check{P}, \hat{P}\}$, *where* Q *is a finite set of states, and* $\check{P}, \hat{P} : Q \times Q \to [0, 1]$ *are functions, with* $\check{P}(q, q')$ *and* $\hat{P}(q, q')$ *representing lower and upper bounds on the probability of transitioning from state* q *to* q', *respectively.*

For all $q \in Q$, we have that $\check{P}(q, q') \leq \hat{P}(q, q')$ and $\sum_{q' \in Q} \check{P}(q, q') \leq 1 \leq \sum_{q' \in Q} \hat{P}(q, q')$. A path of an IMC is a sequence of states $\omega = q_0, q_1, q_2, \ldots$, with $q_i \in Q$. Denote the set of the IMC's finite paths by $Paths^{fin}(\mathrm{S}_{\mathrm{imc}})$. Given a state $q \in Q$, a transition probability distribution $p_q : Q \to [0, 1]$ is called *feasible* if $\check{P}(q, q') \leq p_q(q') \leq \hat{P}(q, q')$ for all $q' \in Q$. Given $q \in Q$, its set of feasible distributions is denoted by Γ_q. We denote by $\Gamma_Q = \{p_q : p_q \in \Gamma_q, q \in Q\}$, the set of all feasible distributions for all states.

Definition II.2 (Adversary): *Given an IMC* S_{imc}, *an* adversary *is a function* $\boldsymbol{\pi} : Paths^{fin}(\mathrm{S}_{imc}) \to \Gamma_Q$, *such that* $\boldsymbol{\pi}(\omega) \in \Gamma_{\omega(end)}$, *i.e., given a finite path it returns a feasible distribution w.r.t. the path's last element.*

The set of all adversaries is denoted by Π. Given a $\boldsymbol{\pi} \in \Pi$ and $\omega(0) = q_0$, an IMC path evolves as follows: at any time-step $i > 0$, $\boldsymbol{\pi}$ chooses a distribution $p \in \Gamma_{\omega(i-1)}$ from which $\omega(i)$ is sampled.

IMCs may be equipped with a reward function $R : Q \to [0, R_{\max}]$. Given a $\boldsymbol{\pi} \in \Pi$ and an initial condition $q_0 \in Q$, all expectations listed in Section II-B are well-defined and single-valued: e.g., $\mathrm{E}^{q_0}_{\boldsymbol{\pi}}[g_{\mathrm{cum},N}(\omega)]$ (see [24]). However, due to the existence of infinite adversaries, the IMC produces whole ranges of such expectations. The bounds of these ranges, e.g., ($\sup_{\boldsymbol{\pi} \in \Pi}$ and) $\inf_{\boldsymbol{\pi} \in \Pi} \mathrm{E}^{q_0}_{\boldsymbol{\pi}}[g_{\mathrm{cum},N}(\omega)]$, can be computed via well-known *value-iteration* algorithms (e.g., see [24], [30]).

III. Sampling Behavior of Stochastic PETC: Framework and Problem Statement

A. Linear Stochastic PETC Systems

Consider a state-feedback stochastic linear control system:

$$d\zeta(t) = A\zeta(t)dt + BK\zeta(t)dt + B_w dW(t)$$

where A, B, K, and B_w are matrices of appropriate dimensions, $\zeta(t) \in \mathbb{R}^{n_\zeta}$ is the state, and $W(t)$ is an n_w-dimensional Wiener process on a complete probability space $(\Omega, \mathcal{F}, \{\mathcal{F}_t\}_{t \geq 0}, \mathbb{P})$. Ω denotes the sample space, $\mathcal{F}$ the σ-algebra generated by W, $\{\mathcal{F}_t\}_{t \geq 0}$ the natural filtration, and $\mathbb{P}$ the probability measure. We denote the solution of the above stochastic differential equation with initial condition ζ_0 by $\zeta(t; \zeta_0)$.

In PETC, the control input is held constant between consecutive *sampling times* (or *event times*) t_i, t_{i+1} and is only updated on such times

$$d\zeta(t) = A\zeta(t)dt + BK\zeta(t_i)dt + B_w dW(t), \quad t \in [t_i, t_{i+1}). \tag{1}$$

Sampling times are determined by the *triggering condition:*

$$t_{i+1} = t_i + \min \Big\{ \overline{k}h, \min \{kh : k \in \mathbb{N}, \phi(\zeta(kh; \zeta(t_i)), \zeta(t_i)) > 0\} \Big\} \tag{2}$$

where $t_0 = 0$, $h > 0$ is a *checking period*, $\overline{k} \in \mathbb{N}_+$, ϕ is called *triggering function*, and $t_{i+1} - t_i$ is called *intersampling time*. PETC works as follows during an intersampling interval $[t_i, t_{i+1})$: At time t_i, the triggering function $\phi(\zeta(t_i), \zeta(t_i))$ is negative; the sensors, periodically with period h, measure the state and check if the triggering function is positive; if it is found positive, or if $\overline{k}h$ time has elapsed since t_i, a new event t_{i+1} is triggered, the latest state-measurement is sent to the controller, which updates the control action, and the whole process is repeated again. The forced upper-bound $\overline{k}h$ on intersampling times is applied in practice (see, e.g., [14], [31]), to prevent the system from operating in an open-loop manner indefinitely; that is, its presence is a standard assumption from a practical viewpoint. Nonetheless, this assumption can be lifted, as explained in Remark 7. We call the combination (1) and (2) *(stochastic) PETC system.*

Intersampling time is a random variable that depends on the previously measured state and we denote it as follows:

$$\tau(x) = \min \Big\{ \overline{k}h, \min \{kh : k \in \mathbb{N}, \phi(\zeta(kh; x), x) > 0\} \Big\}$$

where $x \in \mathbb{R}^n$ is the previously measured state. Note that, because the system is time-homogeneous, reasoning w.r.t. the interval $[t_i, t_{i+1})$ is equivalent to reasoning w.r.t. $[0, t_{i+1} - t_i)$.

Assumption 1: *We assume the following.*

1) *The matrix pair* (A, B_w) *is controllable.*
2) *The checking period* $h = 1$.
3) $\phi(\zeta(t; x), x) = |\zeta(t; x) - x|_\infty - \epsilon$, *where* $\epsilon > 0$ *is a predefined constant.*

Item 1 enforces that $\zeta(t)$ is a nondegenerate Gaussian random variable (see [26]). Item 2 is for ease of presentation and without loss of generality. Regarding item 3, ϕ is the well-studied Lebesgue-sampling triggering function [10] with an ∞-norm instead of a 2-norm. We restrict to this case for clarity, but our results can be extended to more general functions, as explained in Remark 10.

Remark 1: *As it was shown in [Th. 6.C.2] [32], Lebesgue-sampling guarantees mean-square practical stability for PETC system (1) and (2).*

B. Sampling Behavior and Associated Metrics

A stochastic PETC system may exhibit different sequences of state measurements and intersampling times $(\zeta_0, t_0), (\zeta(t_1), t_1 - t_0), (\zeta(t_2), t_2 - t_1), \ldots$, where t_i are sampling times. We call *sampling behavior*, the set of all possible such sequences:

Definition III.1 (Sampling Behavior): *We call N-sampling behavior of stochastic PETC system (1), (2) the set:*

$$\mathrm{Y}_N = \left\{(x_0, s_0), \ldots, (x_N, s_N) : x_i \in \mathbb{R}^{n_\zeta}, s_i \in \mathbb{N}_{[0,\overline{k}]}\right\} \quad (3)$$

where $N \in \mathbb{N}$. When N is clear from the context, it is omitted.

We denote $Q := \mathbb{R}^{n_\zeta} \times \mathbb{N}_{[0,\overline{k}]}$. Given an initial condition $y_0 = (x_0, s_0) \in Q$, the set Y_N is associated with a probability measure $\mathbb{P}^{y_0}_{\mathrm{Y}_N}$ (conditioned on y_0), which is inductively defined over $\mathcal{B}(\mathrm{Y}_N)$ as follows[3]:

$$\mathbb{P}^{y_0}_{\mathrm{Y}_N}(\omega(0) \in (X, s)) = \mathbb{1}_{(X,s)}(y_0) \quad (4)$$

$$\mathbb{P}^{y_0}_{\mathrm{Y}_N}(\omega(i+1) \in (X', s') \mid \omega(i) = (x_i, s_i)) = \mathbb{P}(\zeta(s_{i+1}; x_i) \in X', \tau(x_i) = s') \quad (5)$$

where $\omega \in \mathrm{Y}_N$, $s, s_i, s' \in \mathbb{N}_{[0,\overline{k}]}$, $x_i \in \mathbb{R}^{n_\zeta}$, $X, X' \subseteq \mathbb{R}^{n_\zeta}$, and we use (X, s), with $s \in \mathbb{N}$, to denote the set $\{(x, s) : x \in X\}$. This measure is well-defined, even when the horizon $N = +\infty$, according to the Ionescu–Tulcea theorem [33].

Remark 2: *As noted in Section III-A, typically it is assumed that the first sampling time $t_0 = 0$, which implies that the first intersampling time $s_0 = t_0 - 0 = 0$ and the initial condition is $y_0 = (x_0, 0)$.*

Remark 3: *Under item 3 of Assumption 1, and in every Zeno-free ETC scheme, $\mathbb{P}(\tau(x) = 0) = 0$ for any $x \in \mathbb{R}^{n_\zeta}$, because the triggering function is strictly negative for $k = 0$. Thus, for any $i \geq 1$ and $\omega \in \mathrm{Y}_N$: $\mathbb{P}_{\mathrm{Y}_N}(\mathbf{proj}_{\mathbb{N}_{[0,\overline{k}]}}(\omega(i)) = 0) = 0$. Note that this is not in contrast with Remark 2 that only reasons about initial conditions (x_0, s_0) and not (x_i, s_i) with $i \geq 1$.*

Studying PETC's sampling behavior may be formalized by defining functions $g : \mathrm{Y}_N \to \mathbb{R}$ and computing their expectations $\mathrm{E}_{\mathbb{P}^{y_0}_{\mathrm{Y}_N}}[g(\omega)]$. Here, we focus on functions that can be described as cumulative $g_{\mathrm{cum},N}$, average $g_{\mathrm{avg},N}$, or multiplicative $g_{\mathrm{mul},N}$ rewards (see Section II-B). By appropriately choosing the reward R, these classes of functions can describe many interesting properties of PETC's sampling behavior:

1) *Example 1:* Consider $R(x, s) = s$. Then, $\mathrm{E}_{\mathbb{P}^{y_0}_{\mathrm{Y}_N}}[g_{\mathrm{avg},N}(\omega)]$ is the expected average intersampling time: The larger it is, the less frequently the system is expected to sample, saving more bandwidth and energy.
2) *Example 2:* Consider $R(x, s) = \alpha\frac{1}{|x|+\varepsilon} + \beta s$, with $\alpha, \beta, \varepsilon > 0$, penalizing paths that overshoot far from the origin or exhibit a high sampling frequency. A bigger $\mathrm{E}_{\mathbb{P}^{y_0}_{\mathrm{Y}_N}}[g_{\mathrm{cum},N}(\omega)]$ implies better performance in terms of stabilization speed and sampling frequency. Observe how incorporating state measurements x in our definition of sampling behavior allows to include control-performance related metrics, apart from sampling-performance metrics.
3) *Example 3:* Consider the reward:

$$R(x, s) = \begin{cases} 0, & \text{if } s = \overline{k} \\ 1, & \text{otherwise.} \end{cases}$$

Then, we have that

$$\mathrm{E}_{\mathbb{P}^{y_0}_{\mathrm{Y}_N}}[g_{\mathrm{mul},N}(\omega)] = \mathbb{P}^{y_0}_{\mathrm{Y}_N}\left(\mathbf{proj}_{\mathbb{N}_{[0,\overline{k}]}}(\omega(i)) \neq \overline{k}, \forall i\right)$$

$\mathrm{E}_{\mathbb{P}^{y_0}_{\mathrm{Y}_N}}[g_{\mathrm{mul},N}(\omega)]$ is the probability that there is no intersampling time $s = \overline{k}$ in the next N events. The smaller it is, the more probable it is that the system samples, at least once in the first N triggers, with intersampling time $s = \overline{k}$, implying that a bigger maximum intersampling time could be used, allowing the system to sample even less frequently and saving more bandwidth.

Observe that, if the initial condition (x_0, s_0) is only known to obey some distribution $p_0 : Q \to [0, 1]$, the expected reward can be described as

$$\mathrm{E}_{\mathbb{P}^{p_0}_{\mathrm{Y}_N}}[g_{\star,N}(\omega)] = \sum_{s_0 \in \mathbb{N}_{[0,\overline{k}]}} \int_{\mathbb{R}^{n_\zeta}} \mathrm{E}_{\mathbb{P}^{(x_0,s_0)}_{\mathrm{Y}_N}}[g_{\star,N}(\omega)] p_0(x_0, s_0) dx_0.$$

Thus, reasoning about individual initial conditions y_0 is sufficient and immediately extends to the general case of random initial conditions.

Overall, defining PETC's sampling behavior Y_N, associating it to its induced probability measure $\mathbb{P}^{y_0}_{\mathrm{Y}_N}$ given in (4), (5), and studying expectations $\mathrm{E}_{\mathbb{P}^{y_0}_{\mathrm{Y}_N}}[g(\omega)]$ constitutes a formal framework for the study of PETC's sampling behavior.

C. Problem Statement

Unfortunately, exact computation of $\mathrm{E}_{\mathbb{P}^{y_0}_{\mathrm{Y}_N}}[g_{\star,N}(\omega)]$ is generally infeasible. Among others, how to obtain the measure $\mathbb{P}^{y_0}_{\mathrm{Y}_N}$ over the *uncountable* set of paths Y_N and then integrate over it? Hence, we aim at computing bounds over such expectations:

Problem statement: *Consider the PETC system (1), (2) and its sampling behavior Y_N, for some $N \in \mathbb{N}$. Let Assumption 1 hold. Consider a reward function $R : Q \to [0, R_{\max}]$. For all initial conditions $y_0 \in X \times \mathbb{N}_{[0,\overline{k}]}$, where $X \subset \mathbb{R}^{n_\zeta}$ is a compact hyperrectangle, compute (nontrivial) lower and upper bounds on $\mathrm{E}_{\mathbb{P}^{y_0}_{\mathrm{Y}_N}}[g_{\star,N}(\omega)]$, where $\star \in \{cum, avg, mul\}$.*

[3]Consider Q^{N+1} endowed with its product topology. Then, $\mathcal{B}(\mathrm{Y}_N)$ is the σ-algebra generated by cylinder sets of Q^{N+1}.

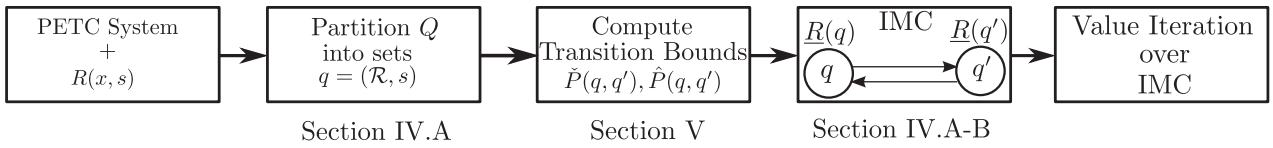

Fig. 1. Flowchart showing the steps followed to compute bounds on the expected rewards $\mathrm{E}_{\mathbb{P}^{y_0}_{\mathrm{Y}_N}}[g_{\star,N}(\omega)]$.

In the rest of this article, we address the problem by constructing an IMC that *abstracts* the sampling behavior Y_N along with $\mathbb{P}^{y_0}_{\mathrm{Y}_N}$, equipping it with suitable reward functions $\underline{R}, \overline{R}$, and computing $(\sup_{\boldsymbol{\pi}\in\Pi}$ and) $\inf_{\boldsymbol{\pi}\in\Pi}\mathrm{E}^{q_0}_{\boldsymbol{\pi}}[g_{\star,N}(\tilde{\omega})]$, with $\star\in\{\mathrm{cum},\mathrm{avg},\mathrm{mul}\}$, to obtain the bounds we are looking for. Specifically, in the next section we show how to construct such an IMC, by partitioning the state space X and providing conditions (7), (8) that have to be satisfied by the IMC's transition probability intervals. We prove in Theorem IV.1 that this IMC equipped with suitable rewards gives rise to bounds on $\mathrm{E}_{\mathbb{P}^{y_0}_{\mathrm{Y}_N}}[g_{\star,N}(\omega)]$. Later, in Section V, we show how to compute $\check{P}$ and $\hat{P}$ such that they satisfy (7) and (8), by solving optimization problems with log-concave objective functions. Finally, the desired bounds $(\sup_{\boldsymbol{\pi}\in\Pi}$ and) $\inf_{\boldsymbol{\pi}\in\Pi}\mathrm{E}^{q_0}_{\boldsymbol{\pi}}[g_{\star,N}(\tilde{\omega})]$ are obtained via well-known value iteration algorithms, as demonstrated through a numerical example in Section VI. A flowchart of the steps followed to compute the desired bounds is shown in Fig. 1.

Remark 4: *By assuming that $y_0=(x_0,s_0)\in X\times\mathbb{N}_{[0,\overline{k}]}$, we essentially assume that the initial state of the system $x_0\in X$. Compactness of X is vital, to partition it into a finite number of subsets $\mathcal{R}_i$ and end up with a finite-state IMC. Nonetheless, this is not an unrealistic assumption, as in practice the initial conditions of the system are usually known to be bounded in some set. X being hyperrectnagular allows us to exactly partition it into hyperrectangles $\mathcal{R}_i$, which facilitates computation of the Gaussian integrals in Section V. If X were not a hyperrectangle, we could still derive a partition into hyperrectangles $\mathcal{R}_i$, such that $X\subseteq\bigcup_i\mathcal{R}_i$, and all results are still valid. Finally, $s_0\in\mathbb{N}_{[0,\overline{k}]}$ for generality, but, as mentioned in Remark 2, typically in ETC $s_0=0$.*

Remark 5: *We constrain ourselves to $\{cum, avg, mul\}$ rewards for clarity, but our approach extends to a more general framework. As commented in Section IV-B, our IMCs can be employed for computing bounds on* bounded-until *probabilities*

$$\mathbb{P}^{y_0}_{\mathrm{Y}_N}(\exists i\in\mathbb{N}_{[0,N]}\text{ s.t. }\omega(i)\in G\text{ and }\forall k\leq i,\omega(k)\in S)$$

where $S,G\subseteq Q$. Since all PCTL formulas can be written with bounded-until operations, our approach covers PCTL. Moreover, by extending our proofs according to [27], we could incorporate probabilistic Linear Temporal Logic (LTL).

IV. IMCs Abstracting PETC's Sampling Behavior

A. Constructing the IMC

Typically, to abstract a stochastic behavior Y and its probability measure $\mathbb{P}_{\mathrm{Y}}$ through an IMC: 1) the state space is partitioned into a finite number of regions, each of which corresponds to an IMC-state, 2) if the state space is unbounded, then one of these regions is unbounded, and its IMC-state is made absorbing,[4] and 3) the bounds on transition probabilities $\check{P}(q,q'),\hat{P}(q,q')$ are derived such that $\check{P}(q,q')\leq\mathbb{P}_{\mathrm{Y}}(\omega(i+1)\in q'|\omega(i)=x)\leq\hat{P}(q,q')$ for all $x\in q$, where $\omega\in\mathrm{Y}$.

We adopt the above methodology. Observe that the state space from which the sampling behavior emerges is the set $Q=\mathbb{R}^{n_\zeta}\times\mathbb{N}_{[0,\overline{k}]}$. Since $\mathbb{N}_{[0,\overline{k}]}$ is by-construction partitioned into the singletons $\{0\},\{1\},\ldots,\{\overline{k}\}$, it suffices to partition $\mathbb{R}^{n_\zeta}$. Consider m nonoverlapping compact hyperrectangles $\mathcal{R}_i$ such that $\bigcup_{i\in\mathbb{N}_{[1,m]}}\mathcal{R}_i=X$. Then, $\mathbb{R}^{n_\zeta}$ is partitioned into

$$Q_{\mathcal{R}}\cup\{\overline{X}\}$$

where $Q_{\mathcal{R}}=\{\mathcal{R}_1,\ldots,\mathcal{R}_m\}$. According to the aforementioned methodology, the states of the IMC would be of the form $(q,s)\in(Q_{\mathcal{R}}\cup\{\overline{X}\})\times\mathbb{N}_{[0,\overline{k}]}$. Nonetheless, for compactness of the IMC, we group all states $(\overline{X},s)$ (for $s\in\mathbb{N}_{[0,\overline{k}]}$) that correspond to $\overline{X}$ into a single absorbing state q_{abs}

$$q_{\mathrm{abs}}=\overline{X}\times\mathbb{N}_{[0,\overline{k}]}.$$

From now on, we abusively use $(\mathcal{R}_i,s)$ (resp. q_{abs}) to denote both the corresponding IMC-state and the set $\mathcal{R}_i\times\{s\}$ (resp. $\overline{X}\times\mathbb{N}_{[0,\overline{k}]}$). Finally, the set of the IMC-states is

$$Q_{\mathrm{imc}}=\left(Q_{\mathcal{R}}\times\mathbb{N}_{[0,\overline{k}]}\right)\cup\{q_{\mathrm{abs}}\}. \tag{6}$$

Regarding the transition probability bounds $\check{P}(q,q')$ and $\hat{P}(q,q')$, since we need to bound $\mathbb{P}(\omega(i+1)\in q'|\omega(i)=x)$ for all $x\in q$, by employing (5), we have that for all $(\mathcal{R},k),(\mathcal{S},s)\in Q_{\mathcal{R}}\times\mathbb{N}_{[0,\overline{k}]}$

$$\begin{aligned}
\check{P}\left((\mathcal{R},k),(\mathcal{S},s)\right)&\leq\min_{x\in\mathcal{R}}\mathbb{P}(\zeta(s;x)\in\mathcal{S},\tau(x)=s)\\
\hat{P}\left((\mathcal{R},k),(\mathcal{S},s)\right)&\geq\max_{x\in\mathcal{R}}\mathbb{P}(\zeta(s;x)\in\mathcal{S},\tau(x)=s)\\
\check{P}\left((\mathcal{R},k),q_{\mathrm{abs}}\right)&\leq\sum_{s\in\mathbb{N}_{[0,\overline{k}]}}\min_{x\in\mathcal{R}}\mathbb{P}(\zeta(s;x)\in\overline{X},\tau(x)=s)\\
\hat{P}\left((\mathcal{R},k),q_{\mathrm{abs}}\right)&\geq\sum_{s\in\mathbb{N}_{[0,\overline{k}]}}\max_{x\in\mathcal{R}}\mathbb{P}(\zeta(s;x)\in\overline{X},\tau(x)=s)
\end{aligned} \tag{7}$$

and for all $q'\in Q_{\mathrm{imc}}$

$$\check{P}(q_{\mathrm{abs}},q')=\hat{P}(q_{\mathrm{abs}},q')=\begin{cases}1, & \text{if } q'=q_{\mathrm{abs}}\\ 0, & \text{otherwise.}\end{cases} \tag{8}$$

The computation of $\check{P}$ and $\hat{P}$ such that they satisfy (7) and (8) is addressed in Section V and it involves bounding the solutions to the optimization problems of (7). The summation in the last two

[4] An IMC-state $q\in Q_{\mathrm{imc}}$ is absorbing $\iff\check{P}(q,q)=1$.

inequalities of (7) results from the fact that q_{abs} is a grouping of all states $(\overline{X}, s)$ with $s \in \mathbb{N}_{[0,\overline{k}]}$, while (8) indicates that q_{abs} is indeed absorbing. In view of Remark 3, since we know that $\mathbb{P}(\tau(x) = 0) = 0$, then for any $q \in Q_{\text{imc}}$ and $\mathcal{S} \in Q_{\mathcal{R}}$, it suffices to write $\check{P}(q, (\mathcal{S}, 0)) = \hat{P}(q, (\mathcal{S}, 0)) = 0$; that is, states $(\mathcal{S}, 0)$ only have outgoing transitions and no incoming ones. Finally, we define the IMC that abstracts the sampling behavior as follows:

$$\mathrm{S}_{\text{imc}} = \left(Q_{\text{imc}}, \check{P}, \hat{P}\right) \tag{9}$$

where Q_{imc} is given by (6) and $\check{P}, \hat{P}$ are given by (7) and (8).

To demonstrate how the constructed IMC abstracts the PETC system's sampling behavior, let us relate paths $\omega \in \mathrm{Y}_N$ to paths $\tilde{\omega} \in Paths^{fin}(\mathrm{S}_{\text{imc}})$. First, consider a path ω such that $\omega(i) \notin q_{\text{abs}}$ for all $i \leq N$. Then, this path is related to a path $\tilde{\omega} \in Paths^{fin}(\mathrm{S}_{\text{imc}})$ of the same length, for which $\omega(i) \in \tilde{\omega}(i)$ for all $i \leq N$. Next, consider a path such that $\omega(i) \in q_{\text{abs}}$ for some $i \leq N$ and $\omega(j) \notin q_{\text{abs}}$ for all $j < i$. Then, ω is related to $\tilde{\omega} \in Paths^{fin}(\mathrm{S}_{\text{imc}})$ of the same length, for which $\omega(j) \in \tilde{\omega}(j)$ for all $j \leq i$ and $\tilde{\omega}(k) = q_{\text{abs}}$ for all $k \geq i$. This latter relation indicates that all paths in Y_N that enter $\overline{X}$ (even those that eventually return to X) are mapped to IMC-paths that enter q_{abs} at the same time and stay there.

B. Bounds on Sampling-Behavior Rewards Via IMCs

The IMC described above, if equipped with suitable rewards $\underline{R}, \overline{R}$, can be employed for the computation of lower and upper bounds on $\mathrm{E}_{\mathbb{P}^{y_0}_{\mathrm{Y}_N}}[g_{\star,N}(\omega)]$:

Theorem IV.1: *Consider the IMC S_{imc} given by (9). Define reward functions $\underline{R}, \overline{R} : Q_{imc} \to [0, R_{\max}]$ such that*

$$\underline{R}(q) = \begin{cases} \min\limits_{(x,s)\in q} R(x,s), & \text{if } q \neq q_{\text{abs}} \\ \min\limits_{(x,s)\in \mathbb{R}^{n_\zeta}\times\mathbb{N}_{[1,\overline{k}]}} R(x,s), & \text{if } q = q_{\text{abs}} \end{cases}$$

$$\overline{R}(q) = \begin{cases} \max\limits_{(x,s)\in q} R(x,s), & \text{if } q \neq q_{\text{abs}} \\ \max\limits_{(x,s)\in \mathbb{R}^{n_\zeta}\times\mathbb{N}_{[1,\overline{k}]}} R(x,s), & \text{if } q = q_{\text{abs}} \end{cases} \tag{10}$$

and the associated rewards over paths $\tilde{\omega} \in Paths^{fin}(\mathrm{S}_{imc})$ denoted by $\underline{g}_{\star,N}, \overline{g}_{\star,N}$, where $\star \in \{cum, avg, mul\}$. Then, for any initial condition $y_0 = (x_0, s_0) \in X \times \mathbb{N}_{[0,\overline{k}]}$ and $N \in \mathbb{N}$:

$$\inf_{\boldsymbol{\pi}\in\Pi} \mathrm{E}^{q_0}_{\boldsymbol{\pi}}[\underline{g}_{\star,N}(\tilde{\omega})] \leq \mathrm{E}_{\mathbb{P}^{y_0}_{\mathrm{Y}_N}}[g_{\star,N}(\omega)] \leq \sup_{\boldsymbol{\pi}\in\Pi} \mathrm{E}^{q_0}_{\boldsymbol{\pi}}[\overline{g}_{\star,N}(\tilde{\omega})]$$

where q_0 is such that $y_0 \in q_0$.

Proof Sketch: The above expectations are written as *value functions* defined via *value iteration* (see Lemma IX.1), and mathematical induction over the iteration is employed. For the full proof, see Appendix A. □

Hence, to compute bounds on expectations $\mathrm{E}_{\mathbb{P}^{y_0}_{\mathrm{Y}_N}}[g_{\star,N}(\omega)]$, we equip the IMC (9) with the reward functions $\underline{R}, \overline{R}$ from (10) and compute the expectations $\inf_{\boldsymbol{\pi}\in\Pi} \mathrm{E}^{q_0}_{\boldsymbol{\pi}}[\underline{g}_{\star,N}(\tilde{\omega})]$ and $\sup_{\boldsymbol{\pi}\in\Pi} \mathrm{E}^{q_0}_{\boldsymbol{\pi}}[\overline{g}_{\star,N}(\tilde{\omega})]$. As mentioned in Section II-C, these expectations can be computed via well-known value-iteration algorithms (e.g., see [24]), with polynomial complexity in the number of IMC states. In fact, the value iteration used for $\{\text{cum}, \text{mul}\}$ rewards is given here by (26) and (37), respectively, in the Appendix (the avg reward is the same as cum with $\gamma = 1$, and in the last step we just divide by $N + 1$). Moreover, as bounded-until probabilities on IMCs, and thus PCTL properties, may be expressed by a similar value iteration [23], our proofs can be adapted to show that we can bound bounded-until probabilities defined over Y_N by using the constructed IMC.

Finally, Theorem IV.1 indicates that *the same IMC* can be used to derive bounds for any chosen $\{\text{cum}, \text{avg}, \text{mul}\}$ reward, for any horizon N, and any initial condition $y_0 \in X \times \mathbb{N}_{[0,\overline{k}]}$. It is also worth noting that a proof like that of Theorem IV.1 was missing from the literature on IMC-abstractions [23], [25], [26], [27], where it was (correctly) taken for granted that the quantitative metric (e.g., a reward) evaluated over the IMC bounds the metric evaluated over the original stochastic behavior, due to the way that the transition probabilities are constructed.

Remark 6: *For any $q \in Q_{imc}$, the rewards $\underline{R}$ and $\overline{R}$ serve as conservative estimates of the real reward obtained if the system operates in q. In fact, specifically for q_{abs}, $\underline{R}$ and $\overline{R}$ are* global *lower and upper bounds, respectively, on the actual reward $R(x, s)$ (except for the case $s = 0$, which happens with zero probability, except for initial conditions). Due to this, for states $(\mathcal{R}, s) \in Q_{imc}$ with $\mathcal{R}$ being "near" $\overline{X}$ (i.e., near the boundary of X), which tend to obtain larger transition probabilities to q_{abs}, the lower and upper bounds $\inf_{\boldsymbol{\pi}\in\Pi} \mathrm{E}^{q_0}_{\boldsymbol{\pi}}[\underline{g}_{\star,N}(\tilde{\omega})]$ and $\sup_{\boldsymbol{\pi}\in\Pi} \mathrm{E}^{q_0}_{\boldsymbol{\pi}}[\overline{g}_{\star,N}(\tilde{\omega})]$ are more conservative, compared to when $\mathcal{R}$ is further inside X. This is showcased by Fig. 4. For that reason, in practice, to construct the IMC, it is better to partition a superset $Y \supseteq X$ into regions $\mathcal{R}_i$, so that the regions that comprise X are further inside Y, and the corresponding bounds are not that conservative.*

Remark 7: *To lift the assumption of a forced upper bound $\overline{k}$ on intersampling times, one could slightly adapt the proposed method to construct the IMC as follows.*

1) *Pick an arbitrary $\overline{k}$ and create the IMC states and the transitions between them as described in Section IV-A.*
2) *Create a second absorbing state $q_{\text{abs},2}$, defined as follows:*

$$q_{\text{abs},2} = \mathbb{R}^{n_\zeta} \times \mathbb{N}_{[\overline{k}+1,+\infty)}.$$

3) *The lower bound on transition probabilities from any state $(\mathcal{R}, k) \in Q_{\mathcal{R}} \times \mathbb{N}_{[0,k]}$ to $q_{\text{abs},2}$ has to be computed such that $\check{P}((\mathcal{R}, k), q_{\text{abs},2}) \leq \min_{x\in\mathcal{R}} \mathbb{P}(\tau(x) > \overline{k})$. Thus, we could define*

$$\check{P}\left((\mathcal{R}, k), q_{\text{abs},2}\right) := 1 - \sum_{s\in\mathbb{N}_{[1,\overline{k}]}} \max_{x\in\mathcal{R}} \mathbb{P}(\tau(x) = s)$$

since the right-hand side is a lower bound on $\min_{x\in\mathcal{R}} \mathbb{P}(\tau(x) > \overline{k})$:

$$1 - \sum_{s\in\mathbb{N}_{[1,\overline{k}]}} \max_{x\in\mathcal{R}} \mathbb{P}(\tau(x) = s) \leq 1 - \max_{x\in\mathcal{R}} \mathbb{P}(\tau(x) \leq \overline{k})$$
$$= \min_{x\in\mathcal{R}} \mathbb{P}(\tau(x) > \overline{k}).$$

The upper bound $\hat{P}((\mathcal{R}, k), q_{\text{abs},2})$ is defined similarly. The terms $\max_{x\in\mathcal{R}} \mathbb{P}(\tau(x) = s)$ can be computed via the methods proposed in Section V.

4) *Define the rewards of both q_{abs} and $q_{\mathrm{abs},2}$ as*

$$\underline{R}(q_{\mathrm{abs}}) = \underline{R}(q_{\mathrm{abs},2}) = \min_{(x,s)\in\mathbb{R}^{n_\zeta}\times\mathbb{N}_{[1,+\infty)}} R(x,s)$$

and similarly for $\overline{R}$.

As with q_{abs}, the fact that $q_{\mathrm{abs},2}$ is made absorbing introduces conservativeness, in the sense that the computed bounds $\sup_{\boldsymbol{\pi}\in\Pi}$ and $\inf_{\boldsymbol{\pi}\in\Pi}\mathrm{E}^{q_0}_{\boldsymbol{\pi}}[g_{\star,N}(\tilde{\omega})]$ are less tight. Picking a larger $\overline{k}$ would make the bounds tighter, at the expense of greater computational load.

Remark 8: *Our results extend to infinite horizons (i.e., $N = +\infty$), when the rewards are well defined, as it has already been proven in [28, Th. IV.1]; in fact, the proof for $N = +\infty$ is simpler, as it suffices to consider time-invariant adversaries.*

The only thing that remains is to describe how to compute the transition probability bounds given by (7). This is carried out in the coming section.

V. Computing the Transition Probability Bounds

Here, we compute lower bounds on the minima and upper bounds on the maxima in (7), thus completing the IMC's construction. Through a series of convex relaxations, and employing Proposition V.1 and Lemma V.2, the min/max expressions in (7) are formulated as optimization problems of log-concave functions (in fact, Gaussian integrals) over hyperrectangles, which are straightforward to solve. For the rest of the document, for any $s \in \mathbb{N}_{[1,N]}$, we denote $\zeta_{s,x} = \zeta(s;x)$ and $\tilde{\zeta}_{s,x} = \begin{bmatrix}\zeta_{1,x}^\top & \zeta_{2,x}^\top & \dots & \zeta_{s,x}^\top\end{bmatrix}^\top$. The following statements are instrumental in our derivations.

Proposition V.1: *For any $s \in \mathbb{N}_{[1,N]}$, we have that $\tilde{\zeta}_{s,x} \sim \mathcal{N}(\mu_{\tilde{\zeta}_{s,x}}, \Sigma_{\tilde{\zeta}_{s,x}})$ with $\mu_{\tilde{\zeta}_{s,x}} = \begin{bmatrix}\mathrm{E}(\zeta_{1,x}^\top) & \mathrm{E}(\zeta_{2,x}^\top) & \dots & \mathrm{E}(\zeta_{s,x}^\top)\end{bmatrix}^\top$,*

$$\Sigma_{\tilde{\zeta}_{s,x}} = \begin{bmatrix}\mathrm{Cov}(1,1) & \mathrm{Cov}(1,2) & \dots & \mathrm{Cov}(1,s)\\ \vdots & \vdots & \dots & \vdots \\ \mathrm{Cov}(s,1) & \mathrm{Cov}(s,2) & \dots & \mathrm{Cov}(s,s)\end{bmatrix}$$

where $\mathrm{E}(\zeta(t;x)) = (e^{At}(I + A^{-1}BK) - A^{-1}BK)x$ and

$$\mathrm{Cov}(t_1,t_2) = \int_0^{\min(t_1,t_2)} e^{A(t_1-s)} B_w B_w^\top e^{A^\top(t_2-s)} ds.$$

Thus, given some set $S \subseteq \mathbb{R}^{sn_\zeta}$, the following holds:

$$\mathbb{P}(\tilde{\zeta}_{s,x} \in S) = \int_S \mathcal{N}(dz|\mu_{\tilde{\zeta}_{s,x}}, \Sigma_{\tilde{\zeta}_{s,x}}). \tag{11}$$

Proof: Application of the expectation and covariance operators to the solution of linear SDE (1) (see [34, pp. 96]). □

Lemma V.2: *Consider a function $h : \mathbb{R}^n \to [0,1]$ with $n \in \mathbb{N}_+$ defined by*

$$h(x) = \int_{S(x)} \mathcal{N}(dz|f(x),\Sigma)$$

where Σ is a covariance matrix, $S(x) \subseteq \mathbb{R}^m$ with $m \in \mathbb{N}_+$ is linear on x and convex for all $x \in \mathbb{R}^n$, and $f : \mathbb{R}^n \to \mathbb{R}^m$ is an affine function. The function $h(x)$ is log concave.

Proof: See Appendix B. □

In what follows, we transform the probabilities involved in (7) to set-membership ones $\mathbb{P}(\tilde{\zeta}_{s,x} \in S(x))$, where $S(x)$ is a polytope, but neither necessarily convex nor linear on x. Afterward, we break them down to simpler ones and employ some convex relaxations, such that the set of integration of the resulting Gaussian integrals is convex and linear on x and Lemma V.2 is enabled. Finally, we end up with optimization problems of log-concave functions over the hyperrectangle $\mathcal{R}$, and solve them to obtain lower and upper bounds on the expressions in (7).

A. Transition Probabilities as Set-Membership Probabilities

For now, let us focus on transitions from any state $(\mathcal{R},k) \in Q_{\mathrm{imc}} \setminus q_{\mathrm{abs}}$ to any state $(\mathcal{S},s) \in Q_{\mathcal{R}} \times \mathbb{N}_{[1,\overline{k}]}$

$$\left(\max_{x\in\mathcal{R}} \text{ or } \right) \quad \min_{x\in\mathcal{R}} \mathbb{P}(\zeta(s;x) \in \mathcal{S}, \tau(x) = s).$$

Later, in Section V-D, we show how transitions to q_{abs} can be treated similarly to the case above. Moreover, remember that for $s = 0$ the above probability is trivially 0 (see Remark 3).

Define the following hyperrectangle:

$$\Phi(x) := \{y \in \mathbb{R}^n : \phi(y,x) \le 0\} = \{y \in \mathbb{R}^n : |y - x|_\infty \le \epsilon\}.$$

Note that $\Phi(x)$ is convex and linear on x: $\Phi(x) = \Phi(0) + \{x\}$. Moreover, it is such that $\zeta(t;x) \in \Phi(x) \iff \phi(\zeta(t;x),x) \le 0$. Thus, the following equivalences hold:

$$\text{if } s \in \mathbb{N}_{[1,\overline{k}-1]} : \tau(x) = s \iff \tilde{\zeta}_{s,x} \in \Phi^{s-1}(x) \times \overline{\Phi}(x)$$

$$\text{if } s = \overline{k} : \tau(x) = s = \overline{k} \iff \tilde{\zeta}_{\overline{k}-1,x} \in \Phi^{\overline{k}-1}(x)$$

where, for brevity, in the case where $s = 1$ we have abusively denoted $\Phi^0(x) \times \overline{\Phi}(x) = \overline{\Phi}(x)$. In other words, when $s \neq \overline{k}$, the intersampling time is s if and only if the state belongs to $\Phi(x)$ at all checking times $1, 2, \dots, s-1$ and at time s it lies outside $\Phi(x)$. When $s = \overline{k}$, it suffices that the state belongs to $\Phi(x)$ at all checking times $1, 2, \dots, \overline{k} - 1$. Thus, applying Proposition V.1, for $s \in \mathbb{N}_{[1,\overline{k}-1]}$:

$$\begin{aligned}&\mathbb{P}(\zeta(s;x) \in \mathcal{S}, \tau(x) = s)\\ &\quad= \mathbb{P}\left(\tilde{\zeta}_{s,x} \in \Phi^{s-1}(x) \times \left(\overline{\Phi}(x) \cap \mathcal{S}\right)\right)\\ &\quad= \int_{\Phi^{s-1}(x)\times(\overline{\Phi}(x)\cap\mathcal{S})} \mathcal{N}\left(dz|\mu_{\tilde{\zeta}_{s,x}}, \Sigma_{\tilde{\zeta}_{s,x}}\right)\end{aligned} \tag{12}$$

and for $s = \overline{k}$:

$$\begin{aligned}\mathbb{P}(\zeta(\overline{k};x) \in \mathcal{S}, \tau(x) = \overline{k}) &= \mathbb{P}\left(\tilde{\zeta}_{\overline{k},x} \in \Phi^{\overline{k}-1}(x) \times \mathcal{S}\right)\\ &= \int_{\Phi^{\overline{k}-1}(x)\times\mathcal{S}} \mathcal{N}\left(dz|\mu_{\tilde{\zeta}_{\overline{k},x}}, \Sigma_{\tilde{\zeta}_{\overline{k},x}}\right).\end{aligned} \tag{13}$$

In the following we combine (12) and (13) with some convex relaxations, to enable Lemma V.2 and obtain bounds on $(\max_{x\in\mathcal{R}}$

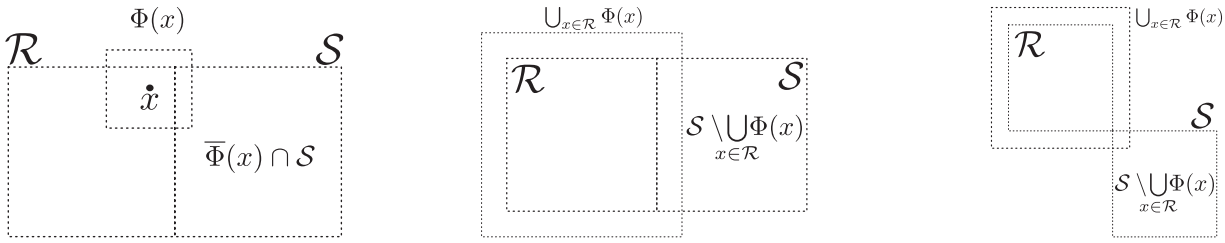

(a) (b) (c)

Fig. 2. Interplay between sets $\mathcal{R}$, $\mathcal{S}$, $\overline{\Phi}(x) \cap \mathcal{S}$ and $\mathcal{S} \setminus \bigcup_{x\in\mathcal{R}} \Phi(x)$. (a) Set $\mathcal{R}$ is the dashed square on the left, $\mathcal{S}$ is the one on the right, and $\Phi(x)$ is the one centered at x. For the given x on the figure, $\overline{\Phi}(x) \cap \mathcal{S}$ is nonconvex. For different $x \in \mathcal{R}$ the set $\overline{\Phi}(x) \cap \mathcal{S}$ has a different shape; thus, $\overline{\Phi}(x) \cap \mathcal{S}$ is not linear on x. (b) Set $\bigcup_{x\in\mathcal{R}} \Phi(x)$, and consequently $\mathcal{S} \setminus \bigcup_{x\in\mathcal{R}} \Phi(x)$, does not depend on x. The set $\mathcal{S} \setminus \bigcup_{x\in\mathcal{R}} \Phi(x)$ can be partitioned into a finite number (minimum one, here) of hyperrectangles. (c) Set $\mathcal{S} \setminus \bigcup_{x\in\mathcal{R}} \Phi(x)$ can be partitioned into a finite number (minimum two, here) of hyperrectangles.

and) $\min_{x\in\mathcal{R}} \mathbb{P}(\zeta(s;x) \in \mathcal{S}, \tau(x) = s)$ through solving optimization problems with log-concave functions. In particular, observe that $\mu_{\tilde{\zeta}_{s,x}}$ is already an affine function of x (see Proposition V.1), thus satisfying one of the two conditions of Lemma V.2. Hence, our efforts focus on transforming the integration sets in (12) and (13) such that they become linear on x and convex.

B. Lower Bounds on Transition Probabilities

Let us start by determining lower bounds on

$$\min_{x\in\mathcal{R}} \mathbb{P}(\zeta(s;x) \in \mathcal{S}, \tau(x) = s). \tag{14}$$

The special case when $s = \overline{k}$, which is given by (13), is simple. Observe that the set $\Phi^{\overline{k}-1}(x) \times \mathcal{S}$ is convex (since $\Phi(x)$ and $\mathcal{S} \in Q_{\mathcal{R}}$ are hyperrectangles) and linear on x, as it can be written as

$$\Phi^{\overline{k}-1}(x) \times \mathcal{S} = \Phi^{\overline{k}-1}(0) \times \mathcal{S} + \begin{bmatrix} I_{n_\zeta} & I_{n_\zeta} & \dots & I_{n_\zeta} & 0_{n_\zeta} \end{bmatrix}^\top \{x\}.$$

Thus, when $s = \overline{k}$, the objective function $\mathbb{P}(\zeta(s;x) \in \mathcal{S}, \tau(x) = s)$ of minimization problem (14) is log-concave (due to (13) and Lemma V.2). The constraint set $\mathcal{R}$ is a hyperrectangle. Thus, the minimization problem attains its solution at one of the vertices of $\mathcal{R}$ [35, pp. 343, Th. 32.2]; we simply have to evaluate the objective function for each of the vertices, to find the minimum.

When $s \neq \overline{k}$, the set of integration in (12) is neither convex nor linear on x due to $\overline{\Phi}(x) \cap \mathcal{S}$ (see Fig. 2(a)); thus, we cannot invoke Lemma V.2 and there is no indication that it is straightforward to compute (14). In this case, we resort to convex relaxations, each of which yield a lower bound on (14) that can be computed easily. These are the following.

a) Relaxation 1: Notice that $\overline{\Phi}(x) \cap \mathcal{S} = \mathcal{S} \setminus \Phi(x)$, for any $x \in \mathcal{R}$. Since $\Phi(x) \subseteq \bigcup_{x\in\mathcal{R}} \Phi(x)$ for all x, it follows that:

$$\overline{\Phi}(x) \cap \mathcal{S} = \mathcal{S} \setminus \Phi(x) \supseteq \mathcal{S} \setminus \bigcup_{x\in\mathcal{R}} \Phi(x).$$

For examples of $\mathcal{S} \setminus \bigcup_{x\in\mathcal{R}} \Phi(x)$, see Fig. 2(b) and (c). Observe that, since $\bigcup_{x\in\mathcal{R}} \Phi(x)$ does not depend on x, the set $\mathcal{S} \setminus \bigcup_{x\in\mathcal{R}} \Phi(x)$ does not depend on x; it is a fixed set, in contrast to $\overline{\Phi}(x) \cap \mathcal{S}$. Moreover, since both $\mathcal{S}$ and $\bigcup_{x\in\mathcal{R}} \Phi(x)$ are hyperrectangles, then $\mathcal{S} \setminus \bigcup_{x\in\mathcal{R}} \Phi(x)$ can always be partitioned into a finite number of hyperrectangles $\mathcal{S}_1, \dots, \mathcal{S}_r$, where $r \leq n$ and $r = 0$ in the case where $\mathcal{S} \setminus \bigcup_{x\in\mathcal{R}} \Phi(x)$ is empty. Thus

$$\begin{aligned} &\min_{x\in\mathcal{R}} \int_{\Phi^{s-1}(x)\times(\overline{\Phi}(x)\cap\mathcal{S})} \mathcal{N}\left(dz|\mu_{\tilde{\zeta}_{s,x}}, \Sigma_{\tilde{\zeta}_{s,x}}\right) \\ &\geq \min_{x\in\mathcal{R}} \int_{\Phi^{s-1}(x)\times(\mathcal{S}\setminus\bigcup_{x\in\mathcal{R}}\Phi(x))} \mathcal{N}\left(dz|\mu_{\tilde{\zeta}_{s,x}}, \Sigma_{\tilde{\zeta}_{s,x}}\right) \\ &\geq \sum_{i=1}^{r} \min_{x\in\mathcal{R}} \int_{\Phi^{s-1}(x)\times\mathcal{S}_i} \mathcal{N}\left(dz|\mu_{\tilde{\zeta}_{s,x}}, \Sigma_{\tilde{\zeta}_{s,x}}\right). \end{aligned} \tag{15}$$

The integration sets $\Phi^{s-1}(x) \times \mathcal{S}_i$ are convex and linear on x. Thus, in the last expression of (15) we are dealing with log-concave objective functions, and r minimization problems attain their minimum at vertices of $\mathcal{R}$. Hence, we easily solve the r minimization problems to obtain a lower bound on (14).

b) Relaxation 2: Here, we employ the law of total probability to write

$$\begin{aligned} &\mathbb{P}\left(\tilde{\zeta}_{s,x} \in \Phi^{s-1}(x) \times (\overline{\Phi}(x) \cap \mathcal{S})\right) \\ &= \mathbb{P}\left(\tilde{\zeta}_{s,x} \in \Phi^{s-1}(x) \times \mathcal{S}\right) - \mathbb{P}\left(\tilde{\zeta}_{s,x} \in \Phi^{s-1}(x) \times (\Phi(x) \cap \mathcal{S})\right) \end{aligned}$$

which gives the following relationship:

$$\begin{aligned} &\min_{x\in\mathcal{R}} \mathbb{P}\left(\tilde{\zeta}_{s,x} \in \Phi^{s-1}(x) \times (\overline{\Phi}(x) \cap \mathcal{S})\right) \\ &\geq \min_{x\in\mathcal{R}} \mathbb{P}\left(\tilde{\zeta}_{s,x} \in \Phi^{s-1}(x) \times \mathcal{S}\right) \\ &\quad - \max_{x\in\mathcal{R}} \mathbb{P}\left(\tilde{\zeta}_{s,x} \in \Phi^{s-1}(x) \times (\Phi(x) \cap \mathcal{S})\right). \end{aligned} \tag{16}$$

The minimization problem in the right-hand side of (16) is similar to the ones discussed before (log-concave objective function and hyperrectangle constraint set), and the minimum can be computed easily. However, the set $\Phi(x) \cap \mathcal{S}$ not being linear on x makes the maximization problem hard to solve. By employing that $\Phi(x) \cap \mathcal{S} \subseteq \mathcal{S} \cap \bigcup_{x\in\mathcal{R}} \Phi(x)$, we relax it by writing

$$\max_{x\in\mathcal{R}} \mathbb{P}\left(\tilde{\zeta}_{s,x} \in \Phi^{s-1}(x) \times (\Phi(x) \cap \mathcal{S})\right)$$

$$\leq \max_{x\in\mathcal{R}} \mathbb{P}\left(\tilde{\zeta}_{s,x} \in \Phi^{s-1}(x) \times \left(\mathcal{S} \cap \bigcup_{x\in\mathcal{R}} \Phi(x)\right)\right).$$

The set $\mathcal{S} \cap \bigcup_{x\in\mathcal{R}} \Phi(x)$ is a (possibly empty) hyperrectangle and does not depend on x; thus, $\Phi^{s-1}(x) \times (\mathcal{S} \cap \bigcup_{x\in\mathcal{R}} \Phi(x))$ is convex and linear on x. Hence, the maximization problem in the right-hand side of the above equation is a convex program (log-concave objective function over the convex constraint set $\mathcal{R}$), and can be easily solved via regular convex optimization techniques. By computing the exact minimum in the right-hand side of (16) and an upper bound on the maximum-term as discussed here, we obtain a lower bound on (14).

c) Relaxation 3: Continuing from (16), we propose a different relaxation for the maximization problem in the right-hand side of (16). Specifically, by employing Bayes's rule:

$$\max_{x\in\mathcal{R}} \mathbb{P}\left(\tilde{\zeta}_{s,x} \in \Phi^{s-1}(x) \times (\Phi(x) \cap \mathcal{S})\right)$$
$$\leq \max_{x\in\mathcal{R}} \mathbb{P}\left(\tilde{\zeta}_{s,x} \in \Phi^{s}(x) | \zeta_{s,x} \in \mathcal{S}\right) \cdot \max_{x\in\mathcal{R}} \mathbb{P}(\zeta_{s,x} \in \mathcal{S}). \quad (17)$$

The term $\max_{x\in\mathcal{R}} \mathbb{P}(\zeta_{s,x} \in \mathcal{S})$ can be computed exactly easily, as $\mathbb{P}(\zeta_{s,x} \in \mathcal{S})$ is log-concave on x. For the term $\max_{x\in\mathcal{R}} \mathbb{P}(\tilde{\zeta}_{s,x} \in \Phi^{s}(x) | \zeta_{s,x} \in \mathcal{S})$, we make use of the following bound.

Proposition V.3: *The following holds:*

$$\max_{x\in\mathcal{R}} \mathbb{P}\left(\tilde{\zeta}_{s,x} \in \Phi^{s}(x) | \zeta_{s,x} \in \mathcal{S}\right)$$
$$\leq \max_{(x,v)\in\mathcal{R}\times\mathcal{S}} \mathbb{P}\left(\tilde{\zeta}_{s,x} \in \Phi^{s}(x) | \zeta_{s,x} = v\right). \quad (18)$$

Proof: The proof is the same as in [36, Lemma II]. □

To compute the right-hand side of (18), we use the fact that the random variable $\xi = (\tilde{\zeta}_{s,x} | \zeta_{l,x} = v)$ is normally distributed.

Corollary V.4 (Proposition V.1): *Consider the random variable $\xi = (\tilde{\zeta}_{s,x} | \zeta_{l,x} = v)$, where $l \in \mathbb{N}_{[1,s]}$, and $v \in \mathbb{R}^n$. Then $\xi \sim \mathcal{N}(\mu_\xi(x,v), \Sigma_\xi)$, where*

$$\mu_\xi(x,v) = \mathrm{E}(\tilde{\zeta}_{s,x}) - \Sigma_{\tilde{\zeta}_{s,x},\zeta_{l,x}} \Sigma^{-1}_{\zeta_{l,x}} (v - \mathrm{E}(\zeta_{l,x}))$$
$$\Sigma_\xi = \Sigma_{\tilde{\zeta}_{s,x}} - \Sigma_{\tilde{\zeta}_{s,x},\zeta_{l,x}} \Sigma^{-1}_{\zeta_{l,x}} \Sigma_{\zeta_{l,x},\tilde{\zeta}_{s,x}}$$

where $\Sigma_{\zeta_{l,x}} = Cov(l,l)$, $\Sigma_{\tilde{\zeta}_{s,x}}$, $\mathrm{E}(\tilde{\zeta}_{s,x})$, and $\mathrm{E}(\zeta_{l,x})$ are obtained from Proposition V.1, and $\Sigma_{\zeta_{l,x},\tilde{\zeta}_{s,x}} = \Sigma^\top_{\tilde{\zeta}_{s,x},\zeta_{l,x}} = \begin{bmatrix} Cov(l,1) & Cov(l,2) & \dots & Cov(l,s) \end{bmatrix}$.

Proof: Straightforward application of the well-known formula for conditional normal distributions [37]. □

Thus, we have that

$$\max_{(x,v)\in\mathcal{R}\times\mathcal{S}} \mathbb{P}\left(\tilde{\zeta}_{s,x} \in \Phi^{s}(x) | \zeta_{s,x} = v\right)$$
$$= \max_{(x,v)\in\mathcal{R}\times\mathcal{S}} \int_{\Phi^s(x)} \mathcal{N}(dz | \mu_\xi(x,v), \Sigma_\xi).$$

Observe that $\mu_\xi(x,v)$ is affine on the optimization variables (x,v), and $\Phi^s(x)$ is obviously convex and linear on x. Thus, the objective function of the above maximization problem is log-concave. Finally, since the set of constraints $\mathcal{R} \times \mathcal{S}$ is convex, we deduce that computing the right-hand side of (18) is a convex program. Combining (18) with (17) and (16) yields an easily computable bound on (14).

Remark 9: *Gaussian integrals over hyperrectangles are often encountered in fields such as statistics and learning, and many algorithms exist for their numerical computation (e.g., Genz's algorithm [38] or python's* scipy.stats.multivariate_normal *[39]).*

Finally, when computing the IMC's transition bounds, the least conservative among the lower bounds obtained by the above three relaxations, i.e., the largest one, is chosen to serve as the lower bound on (14), which determines the lower bounds on transition probabilities $\check{P}((\mathcal{R},k),(\mathcal{S},s))$. From the experiments we have performed, we observed that which of the relaxations yields a better bound depends on the particular case of $\mathcal{R}$, $\mathcal{S}$, and s; thus, we have presented them all.

C. Upper Bounds on Transition Probabilities

We proceed to computing upper bounds on

$$\max_{x\in\mathcal{R}} \mathbb{P}(\zeta(s;x) \in \mathcal{S}, \tau(x) = s). \quad (19)$$

Again, the case where $s = \overline{k}$ is easy: It corresponds to a convex program, and (19) is computed exactly. For the case where $s \neq \overline{k}$, we employ a relaxation similar to Relaxation 3 described in the previous. In particular, as in (16), we write

$$\max_{x\in\mathcal{R}} \mathbb{P}\left(\tilde{\zeta}_{s,x} \in \Phi^{s-1}(x) \times (\overline{\Phi}(x) \cap \mathcal{S})\right)$$
$$\leq \max_{x\in\mathcal{R}} \mathbb{P}\left(\tilde{\zeta}_{s,x} \in \Phi^{s-1}(x) \times \mathcal{S}\right)$$
$$- \min_{x\in\mathcal{R}} \mathbb{P}\left(\tilde{\zeta}_{s,x} \in \Phi^{s-1}(x) \times (\Phi(x) \cap \mathcal{S})\right). \quad (20)$$

The term $\max_{x\in\mathcal{R}} \mathbb{P}(\tilde{\zeta}_{s,x} \in \Phi^{s-1}(x) \times \mathcal{S})$ is computed easily, through convex optimization. For the other term in the right-hand side of (20), we write as in (17)

$$\min_{x\in\mathcal{R}} \mathbb{P}\left(\tilde{\zeta}_{s,x} \in \Phi^{s-1}(x) \times (\Phi(x) \cap \mathcal{S})\right)$$
$$\geq \min_{x\in\mathcal{R}} \mathbb{P}\left(\tilde{\zeta}_{s,x} \in \Phi^{s}(x) | \zeta_{s,x} \in \mathcal{S}\right) \cdot \min_{x\in\mathcal{R}} \mathbb{P}(\zeta_{s,x} \in \mathcal{S}). \quad (21)$$

Given the discussion of the previous section, it is clear that: a) $\min_{x\in\mathcal{R}} \mathbb{P}(\zeta_{s,x} \in \mathcal{S})$ is computed exactly (by traversing the vertices of $\mathcal{R}$), and b) a lower bound on $\min_{x\in\mathcal{R}} \mathbb{P}(\tilde{\zeta}_{s,x} \in \Phi^{s}(x) | \zeta_{s,x} \in \mathcal{S})$ is computed by employing Proposition 5.3 and Corollary 5.4, which yield log-concave minimization over the polytope $\mathcal{R} \times \mathcal{S}$.

D. Transitions to q_{abs}

According to the last two inequalities in (7), for transitions to q_{abs} we are interested in

$$\left(\min_{x\in\mathcal{R}} \text{ or }\right) \quad \max_{x\in\mathcal{R}} \mathbb{P}\left(\zeta(s;x) \in \overline{X}, \tau(x) = s\right).$$

We focus on the maximization, as minimization follows identical steps. By the law of total probability, we have

$$\max_{x\in\mathcal{R}} \mathbb{P}\left(\zeta(s;x)\in\overline{X}, \tau(x)=s\right)$$
$$\leq \max_{x\in\mathcal{R}} \mathbb{P}(\tau(x)=s) - \min_{x\in\mathcal{R}} \mathbb{P}(\zeta(s;x)\in X, \tau(x)=s). \quad (22)$$

Note that, since X is a hyperrectangle, the term $\min_{x\in\mathcal{R}} \mathbb{P}(\zeta(s;x)\in X, \tau(x)=s)$ can be treated exactly as discussed in the previous sections (where X takes the place of $\mathcal{S}$). Regarding $\mathbb{P}(\tau(x)=s)$, we have the following two cases:

a) $s=\overline{k}$*:* In this case

$$\mathbb{P}(\tau(x)=s) = \mathbb{P}\left(\tilde{\zeta}_{s,x}\in\Phi^{s-1}(x)\right).$$

Thus, $\max_{x\in\mathcal{R}} \mathbb{P}(\tau(x)=s) = \max_{x\in\mathcal{R}} \mathbb{P}(\tilde{\zeta}_{s-1,x}\in\Phi^{s-1}(x))$, which can be computed easily (log-concave objective function and hyperrectangular constraint set).

b) $s\neq\overline{k}$*:* In this case, by the law of total probability:

$$\mathbb{P}(\tau(x)=s) = \mathbb{P}\left(\tilde{\zeta}_{s,x}\in\Phi^{s-1}(x)\times\overline{\Phi}(x)\right)$$
$$= \mathbb{P}\left(\tilde{\zeta}_{s-1,x}\in\Phi^{s-1}(x)\right) - \mathbb{P}\left(\tilde{\zeta}_{s,x}\in\Phi^{s}(x)\right)$$

where when $s=1$ we have abusively denoted $\tilde{\zeta}_{0,x}=x$ and $\Phi^0(x)=x$. Thus, we have

$$\max_{x\in\mathcal{R}} \mathbb{P}(\tau(x)=s)$$
$$\leq \max_{x\in\mathcal{R}} \mathbb{P}\left(\tilde{\zeta}_{s-1,x}\in\Phi^{s-1}(x)\right) - \min_{x\in\mathcal{R}} \mathbb{P}\left(\tilde{\zeta}_{s,x}\in\Phi^{s}(x)\right)$$

and both terms in the right-hand side can be computed easily as discussed in the previous sections (log-concave objective functions and hyperrectangular constraint sets).

Remark 10: *To compute the transition probabilities, we have exploited the fact that* $\Phi(x):=\{y\in\mathbb{R}^n : \phi(y,x)\leq 0\}$ *is a hyperrectangle linear on* x*, which is a consequence of the particular form of the triggering function* $\phi(\zeta(t;x),x)=|\zeta(t;x)-x|_\infty-\epsilon$*. To address the more general mixed-triggering function* $\phi(\zeta(t;x),x)=|\zeta(t;x)-x|-\epsilon_1|\zeta(t;x)|-\epsilon_2$*, where now* $\Phi(x)=\{y\in\mathbb{R}^{n_\zeta} : |y-x|-\epsilon_1|y|-\epsilon_2\leq 0\}$ *is neither a hyperrectangle nor linear on* x*, one could use hyperrectangular approximations* $\check{\Phi}(x)$ *and* $\hat{\Phi}(x)$ *of the set* $\Phi(x)$*, such that both of them are linear on* x *and* $\check{\Phi}(x)\subseteq\Phi(x)\subseteq\hat{\Phi}(x)$ *for all* $x\in\mathcal{R}$*. Nonetheless, this would introduce additional conservativeness and computational load.*

VI. Numerical Examples

We, now, demonstrate our theoretical results with a numerical example. Consider a stochastic PETC system (1) and (2) with

$$A=\begin{bmatrix}-4 & 3\\ -2 & 1\end{bmatrix}, B=\begin{bmatrix}1\\0\end{bmatrix}, K=\begin{bmatrix}-2 & 3\end{bmatrix}, B_w=\begin{bmatrix}2.5 & 0\\ 0 & 2.5\end{bmatrix}$$

and $\epsilon=0.25$, $h=0.006$, $\overline{k}=3$. We are interested in assessing the sampling behavior of the system for initial conditions in $X=[-1.2,1.2]^2$. Following Remark 6, we partition $Y=[-2,2]^2$ into 2500 equal rectangles, and construct the IMC as described in the previous.

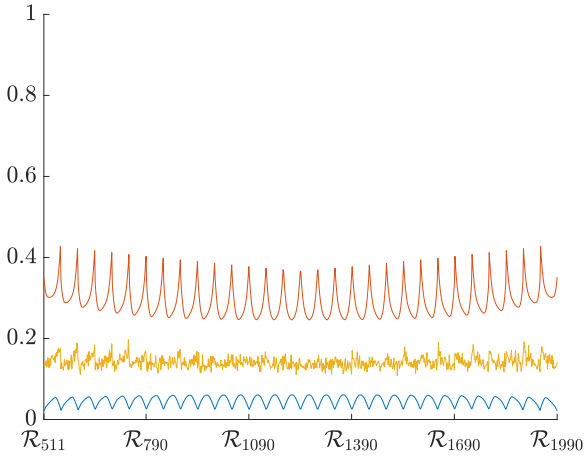

Fig. 3. Blue and red lines are the computed lower and upper bounds, respectively, on the expected multiplicative reward from Example 3 in Section III-B starting from any initial condition $x_0\in\mathcal{R}_i$ (initial intersampling time is assumed $s_0=0$), for all regions $\mathcal{R}_i\subset[-1.2,1.2]^2$ in the partition. The yellow (middle) line is the statistical estimate of the expected reward for a random initial condition from each region.

First, consider the multiplicative reward from Example 3 in Section III-B and a horizon $N=5$. Recall that, in this case, the expected reward expresses the probability that there is no intersampling time $s=\overline{k}$ in the first five triggers. As dictated by Theorem IV.1, we equip the IMC with rewards $\underline{R}$, $\overline{R}$, which are as follows for any $q\in Q_{\text{imc}}$:

$$\underline{R}(q)=\begin{cases}0, & \text{if } q=q_{\text{abs}} \text{ or } \mathbf{proj}_{\mathbb{N}}(q)=\overline{k}\\ 1, & \text{otherwise}\end{cases}$$

$$\overline{R}(q)=\begin{cases}0, & \text{if } \mathbf{proj}_{\mathbb{N}}(q)=\overline{k}\\ 1, & \text{otherwise.}\end{cases}$$

For all $q_0\in Q_{\text{imc}}\setminus q_{\text{abs}}$, we calculate $\inf_{\boldsymbol{\pi}\in\Pi}\mathrm{E}^{q_0}_{\boldsymbol{\pi}}[\underline{g}_{\text{mul},N}(\tilde{\omega})]$ and $\sup_{\boldsymbol{\pi}\in\Pi}\mathrm{E}^{q_0}_{\boldsymbol{\pi}}[\overline{g}_{\text{mul},N}(\tilde{\omega})]$, by employing the value iteration introduced in (37). The adversary that gives rise to each bound is the so-called *o-maximizing MDP* and can be computed easily (see [24] and [23]).

The obtained bounds for all $q_0=(\mathcal{R},0)\in Q_{\mathcal{R}}\times\{0\}$, with $\mathcal{R}\subset[-1.2,1.2]^2$, are shown in Fig. 3. We only consider the case where the initial intersampling time $s_0=0$, as commented in Remark 2.[5] From the obtained bounds, one can expect from the system a high probability of sampling with intersampling time $\overline{k}$. Thus, based on that observation, an engineer who is to implement the PETC system, could decide to further increase the maximum allowed intersampling time, in order to allow the system to sample even less frequently.

Fig. 3, also, shows the statistical estimate of the expected reward, as derived by simulations. Specifically, for all $q_0\in Q_{\mathcal{R}}\times\{0\}$ with $\mathcal{R}\subset[-1.2,1.2]^2$, we pick a random initial condition $y_0\in q_0$ and simulate 1000 sample paths, with a horizon

[5]This is with no loss to generality, as s_0 does not affect the evolution of the system: For different s_0 and the same realization of the Wiener process, the sample path evolves exactly the same.

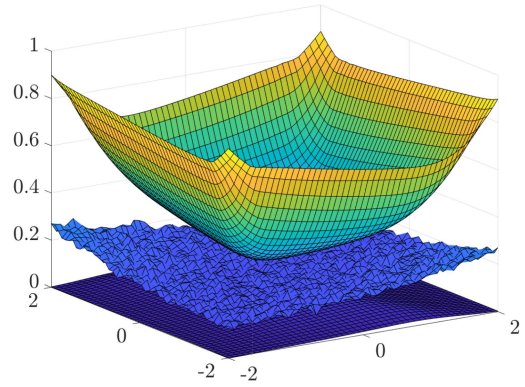

Fig. 4. Surface plot of the obtained lower and upper bounds on the expected multiplicative reward from Example 3 in Section III-B for all regions $\mathcal{R}_i \subset [-2,2]^2$ in the partition (*x*-axis). The surface on the bottom is the lower bound, the surface at the top is the upper bound, and the one in the middle is the statistical estimate of the expected reward for a random initial condition from each region, as obtained from simulations.

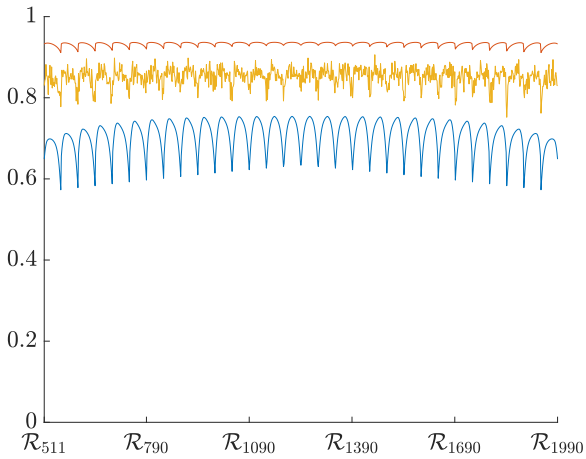

Fig. 5. Blue and red lines are lower and upper bounds, respectively, on the bounded-until probability (23) starting from any initial condition $x_0 \in \mathcal{R}_i$ (initial intersampling time is assumed $s_0 = 0$), for all regions $\mathcal{R}_i \subset [-1.2, 1.2]^2$. The yellow line (the one in the middle) is the statistical estimate of the probability for a random initial condition from each region.

of five triggers (the simulation stops after the fifth trigger). Each sample path that does not generate any intersampling time $s = \overline{k}$ is counted, and the total count is divided by 1000 to obtain a statistical estimate of the true probability. Fig. 3 shows that, as expected by Theorem IV.1, the statistical estimate is confined within the computed bounds. Finally, Fig. 4 is a surface plot illustrating the obtained bounds and the statistical estimate for all regions $\mathcal{R}_i \in [-2,2]^2$, supporting what is discussed in Remark 6: Regions closer to the boundary of the partition correspond to more conservative bounds.

Next, to demonstrate our results' extension to PCTL, we derive bounds on the following bounded-until probability:

$$\mathbb{P}^{y_0}_{Y_N}\left(\exists i \in \mathbb{N}_{[0,5]} \text{ s.t. } \mathbf{proj}_{\mathbb{N}}(\omega(i)) = \overline{k} \right. \\ \left. \text{and } \forall k \leq i, \omega(k) \notin q_{\text{abs}}\right). \tag{23}$$

This is the probability that the state stays in Y *until* there is a trigger $s = \overline{k}$, in a horizon $N = 5$. Fig. 5 shows the results.

Finally, for completeness, we calculate bounds on the expected average intersampling time for $N = 5$, as introduced

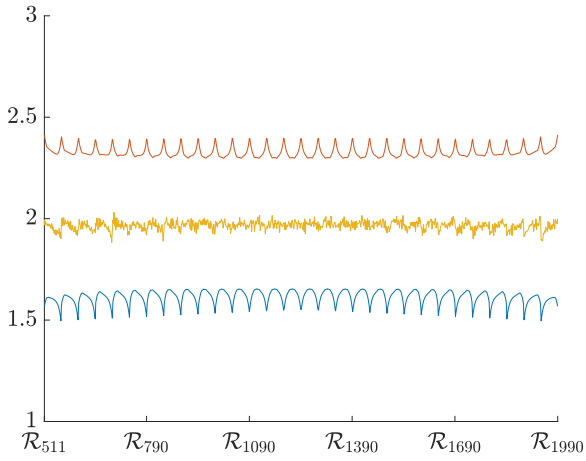

Fig. 6. Blue and red lines are lower and upper bounds on the expected average intersampling time starting from any initial condition $x_0 \in \mathcal{R}_i$ (initial intersampling time is assumed $s_0 = 0$), for regions $\mathcal{R}_i \subset [-1.2, 1.2]^2$. The yellow line (the one in the middle) is the statistical estimate of the expected average for a random initial condition from each region.

in Example 1, Section III-B. Since we assume $s_0 = 0$, which implies that we are only interested in the average of the five subsequent triggers, we use N in the denominator, instead of $N + 1$. The results are illustrated in Fig. 6. The obtained bounds could be used to compare the average sampling performance of this particular PETC design with some other implementation; e.g., it is evident that, on average, it samples considerably more efficiently than a periodic implementation with period h. Alternatively, they could be used to forecast the expected average occupation of the communication channel.

VII. Conclusion

In this work, we have computed bounds on metrics associated with the sampling behavior of linear stochastic PETC systems, by constructing IMCs abstracting the sampling behavior and equipping them with suitable rewards. The metrics are expectations of functions of sequences of intersampling times and state measurements, that take the form of cumulative, average, or multiplicative rewards. Numerical examples have been provided to demonstrate the effectiveness of the proposed framework in practice. Specifically, for a given system, we have computed the expected average intersampling time and the probability of triggering with the maximum allowed intersampling time, in a finite horizon. Moreover, we have computed bounds on a bounded-until probability, demonstrating extensibility of our approach to PCTL properties. Overall, the framework presented here enables the formal study of PETC's sampling behavior and the assessment of its sampling (versus control) performance.

Future work will focus on the following: 1) extending the class of systems considered, as well as addressing the case of continuous ETC, 2) investigating how adaptive partitioning methods or the partition proposed in [16] for deterministic systems can be employed here, for improved and more scalable results, and 3) endowing the IMCs with actions, which will allow for scheduling ETC data traffic in networks shared by multiple

ETC loops, such that performance criteria are met and optimized (e.g., minimizing packet collisions).

APPENDIX

A. Technical Lemmas and Proof of Theorem IV.1

In this section, we first provide some technical lemmas, and then prove Theorem IV.1. Let us introduce some notation and terminology. We constrain ourselves to Markovian adversaries. The value of such adversaries depends only on the time-step i and the given state $q \in Q_{\text{imc}}$, i.e., $\boldsymbol{\pi}(i,q) = p_{i,q} \in \Gamma_q$. From now on, we abusively write $\boldsymbol{\pi}(i,q,q') = p_{i,q}(q')$, for any $q' \in Q_{\text{imc}}$, to denote the transition probability from q to q' at time i, under adversary $\boldsymbol{\pi}$. Moreover, for $s_i, s_{i+1} \in \mathbb{N}_{[0,\overline{k}]}$, $x_i \in \mathbb{R}^{n_\zeta}$, $X_{i+1} \subseteq \mathbb{R}^{n_\zeta}$, denote

$$T((X_{i+1}, s_{i+1})|(x_i, s_i)) := \mathbb{P}^{y_0}_{\mathrm{Y}_N}(\omega(i+1) \in (X_{i+1}, s_{i+1})|\omega(i) = (x_i, s_i)). \quad (24)$$

This notation is common in the literature of stochastic systems and T is often called *transition kernel*. Let us abuse notation and write $\int_Q T(dy'|y)$, for some $y \in Q$, to denote $\sum_{s' \in \mathbb{N}_{[0,\overline{k}]}} \int_{\mathbb{R}^n} T((dx', s')|y)$.

We proceed to stating the technical lemmas. The first one provides a relationship indicating that the expected cumulative reward can be written as a *value function* defined via *value iteration*, which is a trivial extension of the value iteration in [24] to finite horizons and time-varying adversaries. The second and third lemmas provide some useful bounds, which are employed in the Proof of Theorem IV.1.

Lemma IX.1: *Given IMC S_{imc} from (9), equipped with a reward function $\underline{R} : Q_{imc} \to [0, R_{\max}]$, any Markovian adversary $\boldsymbol{\pi} \in \Pi$ and any $q_0 \in Q_{imc}$, we have that*

$$\mathrm{E}_{\boldsymbol{\pi}}\left[\sum_{j=i}^{N} \gamma^{j-i} \underline{R}(\tilde{\omega}(j))|\tilde{\omega}(i) = q_0\right] = \underline{V}_{\boldsymbol{\pi},i}(q_0) \quad (25)$$

where for all $q \in Q_{imc}$ and $i \in \mathbb{N}_{[0,N-1]}$:

$$\underline{V}_{\boldsymbol{\pi},N}(q) = \underline{R}(q) \quad (26a)$$

$$\underline{V}_{\boldsymbol{\pi},i}(q) = \underline{R}(q) + \gamma \sum_{q' \in Q_{\text{imc}}} \underline{V}_{\boldsymbol{\pi},i+1}(q')\boldsymbol{\pi}(i,q,q'). \quad (26b)$$

Similarly, for all $y_0 \in Q$:

$$\mathrm{E}_{\mathbb{P}^{y_0}_{\mathrm{Y}}}\left[\sum_{j=i}^{N} \gamma^{j-i} R(\omega(j))|\omega(i) = y_0\right] = V_i(y_0) \quad (27)$$

where for all $y \in Q$ and $i \in \mathbb{N}_{[0,N-1]}$:

$$V_N(y) = R(y) \quad (28a)$$

$$V_i(y) = R(y) + \gamma \int_Q V_{i+1}(y')T(dy'|y). \quad (28b)$$

Consequently, we have

$$\mathrm{E}^{q_0}_{\boldsymbol{\pi}}\left[\underline{g}_{\text{cum},N}(\tilde{\omega})\right] = \mathrm{E}_{\boldsymbol{\pi}}\left[\sum_{j=0}^{N} \gamma^j \underline{R}(\tilde{\omega}(j))|\tilde{\omega}(0) = q_0\right] = \underline{V}_{\boldsymbol{\pi},0}(q_0)$$

$$\mathrm{E}_{\mathbb{P}^{y_0}_{\mathrm{Y}}}\left[g_{\text{cum},N}(\omega)\right] = \mathrm{E}_{\mathbb{P}^{y_0}_{\mathrm{Y}}}\left[\sum_{j=0}^{N} \gamma^j R(\omega(j))|\omega(0) = y_0\right] = V_0(y_0). \quad (29)$$

Proof: We prove (25) by induction. The proof of (27) is identical, and then (29) follows immediately. It obviously holds that $\underline{V}_{\boldsymbol{\pi},N}(q_0) = R(q_0) = \mathrm{E}_{\boldsymbol{\pi}}[\sum_{j=N}^{N} \gamma^{j-N} \underline{R}(\tilde{\omega}(j))|\tilde{\omega}(N) = q_0]$ for all $q_0 \in Q_{\text{imc}}$. Now, assume that (25) holds for some $i \in \mathbb{N}_{[1,N]}$. Then

$$\begin{aligned}
&\underline{V}_{\boldsymbol{\pi},i-1}(q_0) \\
&= \underline{R}(q_0) + \gamma \sum_{q' \in Q_{\text{imc}}} \underline{V}_{\boldsymbol{\pi},i}(q')\boldsymbol{\pi}(i-1,q_0,q') \\
&= \underline{R}(q_0) + \gamma \sum_{q' \in Q_{\text{imc}}} \mathrm{E}_{\boldsymbol{\pi}}\left[\sum_{j=i}^{N} \gamma^{j-i} \underline{R}(\tilde{\omega}(j))|\tilde{\omega}(i) = q'\right] \\
&\quad \cdot \boldsymbol{\pi}(i-1,q_0,q') \\
&= \underline{R}(q_0) + \mathrm{E}_{\boldsymbol{\pi}}\left[\sum_{j=i}^{N} \gamma^{j-i+1} \underline{R}(\tilde{\omega}(j))|\tilde{\omega}(i-1) = q_0\right] \\
&= \mathrm{E}_{\boldsymbol{\pi}}\left[\underline{R}(q_0) + \sum_{j=i}^{N} \gamma^{j-i+1} \underline{R}(\tilde{\omega}(j))|\tilde{\omega}(i-1) = q_0\right] \\
&= \mathrm{E}_{\boldsymbol{\pi}}\left[\underline{R}(q_0) + \gamma \underline{R}(\tilde{\omega}(i)) + \gamma^2 \underline{R}(\tilde{\omega}(i+1)) \right. \\
&\quad \left. + \ldots |\tilde{\omega}(i-1) = q_0\right] \\
&= \mathrm{E}_{\boldsymbol{\pi}}\left[\sum_{j=i-1}^{N} \gamma^{j-i+1} \underline{R}(\tilde{\omega}(j))|\tilde{\omega}(i-1) = q_0\right]
\end{aligned}$$

where

1) in the second equality, we used the induction assumption that we made;
2) in the third equality we put γ inside the expectation, and we used the law of total expectation;
3) and in the fourth equality, we put $\underline{R}(q_0)$ inside the expectation.

Thus (25) is proven by induction, and the proof is completed. □

Lemma IX.2: *Given any adversary $\boldsymbol{\pi} \in \Pi$, for all $y \in \mathbb{R}^{n_\zeta} \times \mathbb{N}_{[1,\overline{k}]}$ and for all $i \in \mathbb{N}_{[1,N]}$:*

$$\underline{V}_{\boldsymbol{\pi},i}(q_{\text{abs}}) \leq V_i(y). \quad (30)$$

Proof: From Lemma IX.1, we know that

$$V_i(y) = \mathrm{E}_{\mathbb{P}^{y}_{\mathrm{Y}}}\left[\sum_{j=i}^{N} \gamma^{j-i} R(\omega(j))|\omega(i) = y\right]$$

$$\underline{V}_{\boldsymbol{\pi},i}(q_{\text{abs}}) = \mathrm{E}_{\boldsymbol{\pi}}\left[\sum_{j=i}^{N} \gamma^{j-i} \underline{R}(\tilde{\omega}(j))|\tilde{\omega}(i) = q_{\text{abs}}\right]$$

$$= \sum_{j=i}^{N} \gamma^{j-i} \underline{R}(q_{\text{abs}}) = \sum_{j=i}^{N} \gamma^{j-i} \min_{(x,s)\in\mathbb{R}^{n_\zeta}\times\mathbb{N}_{[1,\bar{k}]}} R(x,s) \tag{31}$$

where in the second equation, the second equality comes from the fact that q_{abs} is absorbing for any $\boldsymbol{\pi} \in \Pi$ and the third equality comes from (10).

From Remark 3, since $y \in \mathbb{R}^{n_\zeta} \times \mathbb{N}_{[1,\bar{k}]}$ we can deduce that for all $j \in \mathbb{N}_{[i,N]}$ we have

$$\mathbb{P}_{Y_N}\left(\omega(j) \in \mathbb{R}^{n_\zeta} \times \mathbb{N}_{[1,\bar{k}]} | \omega(i) = y\right) = 1.$$

Thus, we have

$$\min_{(x,s)\in\mathbb{R}^{n_\zeta}\times\mathbb{N}_{[1,\bar{k}]}} R(x,s) \leq R(\omega(j)), \text{for all } j \in \mathbb{N}_{[i,N]} \text{ a.s.} \tag{32}$$

where a.s. means "almost surely." By combining the above equation with (31), (30) follows. □

Lemma IX.3: *Given any adversary* $\boldsymbol{\pi} \in \Pi$ *and any* $y \in Q$*:*

$$\underline{V}_{\boldsymbol{\pi},i}(q_{\text{abs}}) \int_{q_{\text{abs}}} T(dy'|y) \leq \int_{q_{\text{abs}}} V_i(y') T(dy'|y). \tag{33}$$

Proof: We have that

$$\begin{aligned}
&\int_{q_{\text{abs}}} V_i(y') T(dy'|y) \\
&= \int_{\overline{X}\times\mathbb{N}_{[1,\bar{k}]}} V_i(y') T(dy'|y) + \cancelto{0}{\int_{\overline{X}\times\{0\}} V_i(y') T(dy'|y)} \\
&\geq \underline{V}_{\boldsymbol{\pi},i}(q_{\text{abs}}) \int_{\overline{X}\times\mathbb{N}_{[1,\bar{k}]}} T(dy'|y) \\
&= \underline{V}_{\boldsymbol{\pi},i}(q_{\text{abs}}) \int_{\overline{X}\times\mathbb{N}_{[1,\bar{k}]}} T(dy'|y) \\
&\quad + \underline{V}_{\boldsymbol{\pi},i}(q_{\text{abs}}) \underbrace{\int_{\overline{X}\times\{0\}} T(dy'|y)}_{0} \\
&= \underline{V}_{\boldsymbol{\pi},i}(q_{\text{abs}}) \int_{q_{\text{abs}}} T(dy'|y)
\end{aligned}$$

where for crossing out the term $\int_{\overline{X}\times\{0\}} V_i(y') T(dy'|y)$ we used the fact that $\int_{\overline{X}\times\{0\}} T(dy'|y) = 0$ (due to what is discussed in Remark 3), and for the inequality we used Lemma IX.2. □

Now, we are ready to prove Theorem IV.1.

Proof of Theorem IV.1: First, we prove the statement for cumulative rewards, and then we show how the proof is adapted for average and multiplicative rewards. We focus on the lower bound as the proof for the upper bound is similar. It suffices to show that there exists an adversary $\boldsymbol{\pi}^* \in \Pi$ such that

$$\mathrm{E}^{q_0}_{\boldsymbol{\pi}^*}\left[\underline{g}_{\text{cum},N}(\tilde{\omega})\right] \leq \mathrm{E}_{\mathbb{P}^{y_0}_Y}[g_{\text{cum},N}(\omega)]. \tag{34}$$

By employing Lemma IX.1, specifically (29), to prove (34) it suffices to prove that there exists a $\boldsymbol{\pi}^* \in \Pi$ such that for any $q_0 \in Q_{\text{imc}} \setminus \{q_{\text{abs}}\}$ and any $y_0 \in q_0$:

$$\underline{V}_{\boldsymbol{\pi}^*,0}(q_0) \leq V_0(y_0). \tag{35}$$

Consider the following adversary for all $q \in Q_{\text{imc}}, i \in \mathbb{N}_{[0,N-1]}$:

$$\boldsymbol{\pi}^*(i,q,q') = \begin{cases} \int_{q'} T(dy'|y_i^*(q)), & \text{if } q \neq q_{\text{abs}} \\ 1, & \text{if } q = q' = q_{\text{abs}}, \\ 0, & \text{otherwise} \end{cases} \tag{36}$$

where $y_i^*(q) = \arg\min_{y\in q} V_i(y)$. Indeed $\boldsymbol{\pi}^* \in \Pi$, since $\sum_{q'\in Q_{\text{imc}}} \boldsymbol{\pi}^*(i,q,q') = 1$ for all $q \in Q_{\text{imc}}$, and from (7) and (24) it easily follows that $\check{P}(q,q') \leq \boldsymbol{\pi}^*(i,q,q') \leq \hat{P}(q,q')$.[6]

Now, we are ready to prove (35), by induction. First, from (10) it is obvious that $\underline{V}_{\boldsymbol{\pi},N}(q_0) \leq V_N(y_0)$ for any $q_0 \in Q_{\text{imc}} \setminus \{q_{\text{abs}}\}$ and any $y_0 \in q_0$, since

$$\underline{V}_{\boldsymbol{\pi},N}(q_0) = \underline{R}(q_0) \leq R(y_0) = V_N(y_0).$$

Assume that $\underline{V}_{\boldsymbol{\pi},i}(q_0) \leq V_i(y_0)$ for any $q_0 \in Q_{\text{imc}} \setminus \{q_{\text{abs}}\}$ and any $y_0 \in q_0$, for some $i \in \mathbb{N}_{[1,N]}$. Then

$$\begin{aligned}
&\underline{V}_{\boldsymbol{\pi},i-1}(q_0) \\
&= \underline{R}(q_0) + \gamma \sum_{q'\in Q_{\text{imc}}} \underline{V}_{\boldsymbol{\pi},i}(q') \boldsymbol{\pi}(i-1,q_0,q') \\
&= \underline{R}(q_0) + \gamma \sum_{q'\in Q_{\text{imc}}\setminus\{q_{\text{abs}}\}} \underline{V}_{\boldsymbol{\pi},i}(q') \int_{q'} T(dy'|y_{i-1}^*(q_0)) \\
&\quad + \gamma \underline{V}_{\boldsymbol{\pi},i}(q_{\text{abs}}) \int_{q_{\text{abs}}} T(dy'|y_{i-1}^*(q_0)) \\
&\leq \min_{y\in q_0} R(y) + \gamma \sum_{q'\in Q_{\text{imc}}\setminus\{q_{\text{abs}}\}} \min_{y\in q'}(V_i(y)) \int_{q'} T(dy'|y_{i-1}^*(q_0)) \\
&\quad + \gamma \underline{V}_{\boldsymbol{\pi},i}(q_{\text{abs}}) \int_{q_{\text{abs}}} T(dy'|y_{i-1}^*(q_0)) \\
&\leq \min_{y\in q_0} R(y) + \gamma \sum_{q'\in Q_{\text{imc}}\setminus\{q_{\text{abs}}\}} \int_{q'} V_i(y') T(dy'|y_{i-1}^*(q_0)) \\
&\quad + \gamma \int_{q_{\text{abs}}} V_i(y') T(dy'|y_{i-1}^*(q_0)) \\
&\leq R(y_{i-1}^*(q_0)) + \gamma \sum_{q'\in Q_{\text{imc}}} \int_{q'} V_i(y') T(dy'|y_{i-1}^*(q_0)) \\
&= R(y_{i-1}^*(q_0)) + \gamma \int_{Q} V_i(y') T(dy'|y_{i-1}^*(q_0)) \\
&= V_{i-1}(y_{i-1}^*(q_0)) = \min_{y\in q_0} V_{i-1}(y)
\end{aligned}$$

where

1) in the first step we used (26); in the second step we used the definition (36) of $\boldsymbol{\pi}^*$;
2) in the third step, we used that $\underline{R}(q_0) = \min_{y\in q_0} R(y)$ [from (10)] and that $\underline{V}_{\boldsymbol{\pi},i}(q_0) \leq V_i(y_0)$ for any $q_0 \in Q_{\text{imc}} \setminus \{q_{\text{abs}}\}$ and any $y_0 \in q_0$ (from the induction assumption);
3) in the fourth step, we used that $\min_{y\in q'}(V_i(y)) \leq V(y')$ for all $y' \in q'$, and the inequality given by Lemma IX.3;

[6] Adopting the transition-kernel notation, it can be written that for $q \in Q_{\text{imc}} \setminus \{q_{\text{abs}}\}$, $\check{P}(q,q') \leq \min_{y\in q} \int_{q'} T(dy'|y)$, for any $q' \in Q_{\text{imc}}$. Similarly for $\hat{P}$. Indeed it follows that $\check{P}(q,q') \leq \boldsymbol{\pi}^*(i,q,q') \leq \hat{P}(q,q')$.

4) in the sixth step, we used that $\bigcup_{q' \in q_{\text{imc}}} q' = Q$, in the seventh step we used (28), and in the last step we used that $y^*_{i-1}(q_0) = \arg\min_{y \in q_0} V_{i-1}(y)$.

Hence, since $\underline{V}_{\boldsymbol{\pi},i-1}(q_0) \leq \min_{y \in q_0} V_{i-1}(y)$, we have that (35) is proven by induction, thus proving (34).

Only thing remaining is to explain how this proof generalizes to average and multiplicative rewards. The average reward is very simple, as it is just the time-average of a cumulative reward with $\gamma = 1$: $\mathrm{E}[g_{\text{avg},N}(\omega)] = \frac{1}{N+1}\mathrm{E}[\sum_0^N R(\omega(i))]$. Finally, for multiplicative rewards, only thing that changes w.r.t. cumulative rewards is the value iteration, which becomes

$$\underline{V}_{\boldsymbol{\pi},N}(q) = \underline{R}(q)$$
$$\underline{V}_{\boldsymbol{\pi},i}(q) = \underline{R}(q) \cdot \sum_{q' \in Q_{\text{imc}}} \underline{V}_{\boldsymbol{\pi},i+1}(q')\boldsymbol{\pi}(i,q,q'). \tag{37}$$

□

B. Proof of Lemma V.2

Proof of Lemma V.2: This proof draws inspiration from the proof of [40, Proposition II]. Let us first prove log-concavity of the following simpler case:

$$g(x) = \int_S \mathcal{N}(dz|x,\Sigma)$$

with $S \subseteq \mathbb{R}^n$ not dependent on x. Observe that

$$g(x) = \int_{S-\{x\}} \mathcal{N}(dz|0,\Sigma)$$

where $S - \{x\}$ is still a convex set as a mere translation of S. Then, $g(x)$ can be written as

$$g(x) = P(S - \{x\})$$

where $P(\cdot)$ is a probability measure over $\mathcal{B}(\mathbb{R}^n)$ with density $\mathcal{N}(0,\Sigma)$. Since $\mathcal{N}(z|0,\Sigma)$ is log-concave, from [41, Th. 2] we know that P is a log-concave measure, meaning that for every pair of convex sets $S_1, S_2 \subseteq \mathbb{R}^n$ and any $\lambda \in (0,1)$:

$$P(\lambda S_1 + (1-\lambda)S_2) \geq (P(S_1))^{\lambda}(P(S_2))^{1-\lambda}. \tag{38}$$

Moreover, for any $x_1, x_2 \in \mathbb{R}^n$ and any $\lambda \in (0,1)$ we have

$$\begin{aligned}
&\lambda(S - \{x_1\}) + (1-\lambda)(S - \{x_2\}) \\
&\quad = \{\lambda(y - x_1) : y \in S\} + \{(1-\lambda)(w - x_1) : w \in S\} \\
&\quad = \{\lambda(y - x_1) + (1-\lambda)(w - x_1) : y, w \in S\} \\
&\quad = \{\lambda y + (1-\lambda)w - \lambda x_1 - (1-\lambda)x_2 : y, w \in S\} \\
&\quad = \{\lambda y + (1-\lambda)w : y, w \in S\} - \lambda\{x_1\} - (1-\lambda)\{x_2\} \\
&\quad = S - \lambda\{x_1\} - (1-\lambda)\{x_2\}
\end{aligned} \tag{39}$$

where the last equality is because $v = \lambda y + (1-\lambda)w$ is a convex combination of any two points $y, w \in S$ and S is convex.[7]

[7]Since S is convex, then for any two $y, w \in S$ and any $\lambda \in (0,1)$, we have that $v = \lambda y + (1-\lambda)w \in S$. Thus, for a given λ, $\{\lambda y + (1-\lambda)w : y, w \in S\} \subseteq S$. But, also, $S = \{\lambda y + (1-\lambda)y \in S : y \in S\} \subseteq \{\lambda y + (1-\lambda)w : y, w \in S\}$. Thus, it has to be $S = \{\lambda y + (1-\lambda)w : y, w \in S\}$.

Finally, for any $x_1, x_2 \in \mathbb{R}^n$ and any $\lambda \in (0,1)$ we have

$$\begin{aligned}
&g(\lambda x_1 + (1-\lambda)x_2) \\
&\quad = P\left(S - \lambda\{x_1\} + (1-\lambda)\{x_2\}\right) \\
&\quad = P\left(\lambda(S - \{x_1\}) + (1-\lambda)(S - \{x_2\})\right) \\
&\quad \geq \left(P(S - \{x_1\})\right)^{\lambda}\left(P(S - \{x_2\})\right)^{(1-\lambda)} \\
&\quad = (g(x_1))^{\lambda}(g(x_2))^{1-\lambda}
\end{aligned}$$

where in the second equality we used (39) and for the inequality we used (38). Thus, it follows that $g(x)$ is log-concave.

For the general case, since $S(x) \subseteq \mathbb{R}^m$ is linear on x and convex, then it can be written as $S(x) = S' + \{Gx\}$, where $S' \subseteq \mathbb{R}^m$ is convex and $G \in \mathbb{R}^{m \times n}$. Thus, we have

$$\begin{aligned}
h(x) &= \int_{S(x)} \mathcal{N}(dz|f(x),\Sigma) = \int_{S'+\{Gx\}} \mathcal{N}(dz|f(x),\Sigma) \\
&= \int_{S'} \mathcal{N}(dz|f(x) - Gx,\Sigma) \\
&= g(f(x) - Gx)
\end{aligned}$$

where $g(x) = \int_{S'} \mathcal{N}(dz|x,\Sigma)$. The function $h(x) = g(f(x) - Gx)$ is log-concave as the composition of the log-concave function $g(x)$ with the affine function $f(x) - Gx$. □

ACKNOWLEDGMENT

The authors would like to thank Daniel Jarne Ornia and Gabriel de Albuquerque Gleizer for helpful discussions on this work. This work was completed while the Giannis Delimpaltadakis was a Ph.D. candidate at Delft University of Technology.

REFERENCES

[1] P. Tabuada, "Event-triggered real-time scheduling of stabilizing control tasks," *IEEE Trans. Autom. Control*, vol. 52, no. 9, pp. 1680–1685, Sep. 2007.

[2] W. H. Heemels, M. Donkers, and A. R. Teel, "Periodic event-triggered control for linear systems," *IEEE Trans. Autom. Control*, vol. 58, no. 4, pp. 847–861, Apr. 2013.

[3] R. Postoyan, P. Tabuada, D. Nešić, and A. Anta, "A framework for the event-triggered stabilization of nonlinear systems," *IEEE Trans. Autom. Control*, vol. 60, no. 4, pp. 982–996, 2014.

[4] A. Girard, "Dynamic triggering mechanisms for event-triggered control," *IEEE Trans. Autom. Control*, vol. 60, no. 7, pp. 1992–1997, Apr. 2015.

[5] Y. Wang, W. X. Zheng, and H. Zhang, "Dynamic event-based control of nonlinear stochastic systems," *IEEE Trans. Autom. Control*, vol. 62, no. 12, pp. 6544–6551, Dec. 2017.

[6] F. Li and Y. Liu, "Periodic event-triggered output-feedback stabilization for stochastic systems," *IEEE Trans. Cybern.*, vol. 51, no. 10, pp. 5142–5155, Oct. 2021.

[7] Q. Zhu, "Stabilization of stochastic nonlinear delay systems with exogenous disturbances and the event-triggered feedback control," *IEEE Trans. Autom. Control*, vol. 64, no. 9, pp. 3764–3771, Sep. 2019.

[8] S. Luo and F. Deng, "On event-triggered control of nonlinear stochastic systems," *IEEE Trans. Autom. Control*, vol. 65, no. 1, pp. 369–375, Jan. 2020.

[9] B. Demirel, V. Gupta, D. E. Quevedo, and M. Johansson, "On the trade-off between communication and control cost in event-triggered dead-beat control," *IEEE Trans. Autom. Control*, vol. 62, no. 6, pp. 2973–2980, Jun. 2017.

[10] K. J. Astrom and B. M. Bernhardsson, "Comparison of Riemann and Lebesgue sampling for first order stochastic systems," in *Proc. IEEE 41st Conf. Decis. Control*, 2002, pp. 2011–2016.

[11] D. Meister, F. Aurzada, M. A. Lifshits, and F. Allgöwer, "Analysis of time-versus event-triggered consensus for a single-integratormulti-agent system," in *Proc. IEEE 61st Conf. Decis. Control*, 2022, pp. 441–446.
[12] R. Postoyan, R. G. Sanfelice, and W. P. M. H. Heemels, "Inter-event times analysis for planar linear event-triggered controlled systems," in *Proc. IEEE 58th Conf. Decis. Control*, 2019, pp. 1662–1667.
[13] A. Rajan and P. Tallapragada, "Analysis of inter-event times for planar linear systems under a general class of event triggering rules," in *Proc. 59th IEEE Conf. Decis. Control*, 2020, pp. 5206–5211.
[14] G. de A. Gleizer and M. Mazo Jr, "Computing the sampling performance of event-triggered control," in *Proc. 24th Int. Conf. Hybrid Syst., Comput. Control*, 2021, pp. 1–7.
[15] A. S. Kolarijani and M. Mazo Jr, "Formal traffic characterization of LTI event-triggered control systems," *IEEE Trans. Control Netw. Syst.*, vol. 5, no. 1, pp. 274–283, Mar. 2018.
[16] G. d. A. Gleizer and M. Mazo Jr, "Scalable traffic models for scheduling of linear periodic event-triggered controllers," *IFAC-PapersOnLine*, vol. 53, no. 2, pp. 2726–2732, 2020.
[17] G. Delimpaltadakis and M. Mazo Jr, "Traffic abstractions of nonlinear homogeneous event-triggered control systems," in *Proc. IEEE 59th Conf. Decis. Control*, 2020, pp. 4991–4998.
[18] G. Delimpaltadakis and M. Mazo Jr, "Abstracting the traffic of nonlinear event-triggered control systems," *IEEE Trans. Autom. Control*, vol. 68, no. 6, pp. 3744–3751, Jun. 2023.
[19] T. Soleymani, J. S. Baras, and S. Hirche, "Value of information in feedback control: Quantification," *IEEE Trans. Autom. Control*, vol. 67, no. 7, pp. 3730–3737, Jul. 2022.
[20] A. Molin and S. Hirche, "On lqg joint optimal scheduling and control under communication constraints," in *Proc. 48th IEEE Conf. Decis. Control Jointly 28th Chin. Control Conf.*, 2009, pp. 5832–5838.
[21] B. A. Khashooei, D. J. Antunes, and W. Heemels, "A consistent threshold-based policy for event-triggered control," *IEEE Contr. Syst. Lett.*, vol. 2, no. 3, pp. 447–452, Jul. 2018.
[22] L. Mi and L. Mirkin, "H_∞ event-triggered control with performance guarantees vis-á-vis the optimal periodic solution," *IEEE Trans. Autom. Control*, vol. 67, no. 1, pp. 63–74, Jan. 2022.
[23] M. Lahijanian, S. B. Andersson, and C. Belta, "Formal verification and synthesis for discrete-time stochastic systems," *IEEE Trans. Autom. Control*, vol. 60, no. 8, pp. 2031–2045, Aug. 2015.
[24] R. Givan, S. Leach, and T. Dean, "Bounded-parameter Markov decision processes," *Artif. Intell.*, vol. 122, no. 1-2, pp. 71–109, 2000.
[25] M. Dutreix and S. Coogan, "Specification-guided verification and abstraction refinement of mixed monotone stochastic systems," *IEEE Trans. Autom. Control*, vol. 66, no. 7, pp. 2975–2990, Jul. 2021.
[26] L. Laurenti, M. Lahijanian, A. Abate, L. Cardelli, and M. Kwiatkowska, "Formal and efficient synthesis for continuous-time linear stochastic hybrid processes," *IEEE Trans. Autom. Control*, vol. 66, no. 1, pp. 17–32, Jan. 2021.
[27] J. Jackson, L. Laurenti, E. Frew, and M. Lahijanian, "Strategy synthesis for partially-known switched stochastic systems," in *Proc. 24th Int. Conf. Hybrid Syst., Comput. Control*, 2021, pp. 1–11.
[28] G. Delimpaltadakis, L. Laurenti, and M. Mazo Jr, "Abstracting the sampling behaviour of stochastic linear periodic event-triggered control systems," in *Proc. IEEE 60th Conf. Decis. Control*, 2021, pp. 1287–1294.
[29] A. Abate, M. Prandini, J. Lygeros, and S. Sastry, "Probabilistic reachability and safety for controlled discrete time stochastic hybrid systems," *Automatica*, vol. 44, no. 11, pp. 2724–2734, 2008.
[30] M. L. Puterman, *Markov Decision Processes: Discrete Stochastic Dynamic Programming*. Hoboken, NJ, USA: Wiley, 2014.
[31] S. Wildhagen, J. Berberich, M. Hertneck, and F. Allgöwer, "Data-driven analysis and controller design for discrete-time systems under aperiodic sampling," *IEEE Trans. Autom. Control*, vol. 68, no. 6, pp. 3210–225, Jun. 2023.
[32] G. Delimpaltadakis, "Grasping the sampling behaviour of event-triggered control: Self-triggered control, abstractions and formal analysis," PhD thesis, Delft Univ. Technol., 2022.
[33] C. I. Tulcea, "Mesures dans les espaces produits," *Atti Acad. Naz. Lincei Rend. Cl Sci. Fis. Mat. Nat*, vol. 8, no. 7, pp. 208–211, 1949.
[34] X. Mao, *Stochastic Differential Equations and Applications*. New York, NY, USA: Elsevier, 2007.
[35] R. T. Rockafellar, *Convex Analysis*. Princeton, NJ, USA: Princeton Univ. Press, 2015.
[36] A. Blaas, A. Patane, L. Laurenti, L. Cardelli, M. Kwiatkowska, and S. Roberts, "Adversarial robustness guarantees for classification with gaussian processes," 2019, *arXiv:1905.11876*.
[37] M. L. Eaton, *Multivariate Statistics: A Vector Space Approach*. Hoboken, NJ, USA: Wiley, 1983.
[38] A. Genz, "Numerical computation of multivariate normal probabilities," *J. Comput. Graph. Statist.*, vol. 1, no. 2, pp. 141–149, 1992.
[39] P. Virtanen et al., "Scipy 1.0: Fundamental algorithms for scientific computing in python," *Nature Methods*, vol. 17, no. 3, pp. 261–272, 2020.
[40] N. Cauchi, L. Laurenti, M. Lahijanian, A. Abate, M. Kwiatkowska, and L. Cardelli, "Efficiency through uncertainty: Scalable formal synthesis for stochastic hybrid systems," in *Proc. 22nd ACM Int. Conf. Hybrid Syst., Comput. Control*, 2019, pp. 240–251.
[41] A. Prékopa, "On logarithmic concave measures and functions," *Acta Scientiarum Mathematicarum*, vol. 34, pp. 335–343, 1973.

Giannis Delimpaltadakis (Member, IEEE) received the diploma (joint B.Sc. and M.Sc. degrees) in electrical and computer engineering from the National Technical University of Athens, Athens, Greece, in 2017. He received the Ph.D. degree (*cum laude* distinction) from Delft University of Technology, Delft, The Netherlands, in 2022.

He is currently a Postdoctoral Researcher with Eindhoven University of Technology. His research interests include hybrid and stochastic systems, formal methods, and cyber-physical systems.

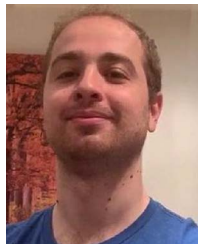

Luca Laurenti received the B.S. degree in information engineering from University La Sapienza, Rome, in 2011, the M.S. degree in information engineering from University of Perugia, Perugia, Italy, in 2013, and the Ph.D. degree from the Department of Computer Science, University of Oxford, Oxford, U.K., in 2018.

He is an Assistant Professor with the Delft Center for Systems and Control at TU Delft and Co-Director of the HERALD DAI Lab. He was a member of Trinity College.

Manuel Mazo Jr. (Senior Member, IEEE) received the M.Sc. and Ph.D. degrees in electrical engineering from the University of California, Los Angeles, CA, USA, in 2007 and 2010, respectively. He also received a telecommunications engineering "Ingeniero" degree from the Polytechnic University of Madrid, Madrid, Spain, and a "Civilingenjör" degree in electrical engineering from the Royal Institute of Technology, Sweden, both awarded in 2003.

He is an Associate Professor with the Delft Center for Systems and Control, Delft University of Technology, The Netherlands. Between 2010 and 2012, he held a joint postdoctoral position with the University of Groningen and the Innovation Centre INCAS3 (The Netherlands). His main research interest is the formal study of problems emerging in modern control system implementations, and in particular the study of networked control systems and the application of formal verification and synthesis techniques to control.

Dr. Mazo has been the recipient of a University of Newcastle Research Fellowship in 2005, the Spanish Ministry of Education/UCLA Fellowship (2005–2009), the Henry Samueli Scholarship from the UCLA School of Engineering and Applied Sciences (2007/2008), and an ERC Starting Grant in 2017.